Experimental signatures of nuclear structure in heavy ion Collisions

Chunjian Zhang

February-07-2023

INSTITUTE for NUCLEAR THEORY

INT PROGRAM INT-23-1A

Intersection of nuclear structure and high-energy nuclear collisions

January 23, 2023 - February 24, 2023

Stony Brook University

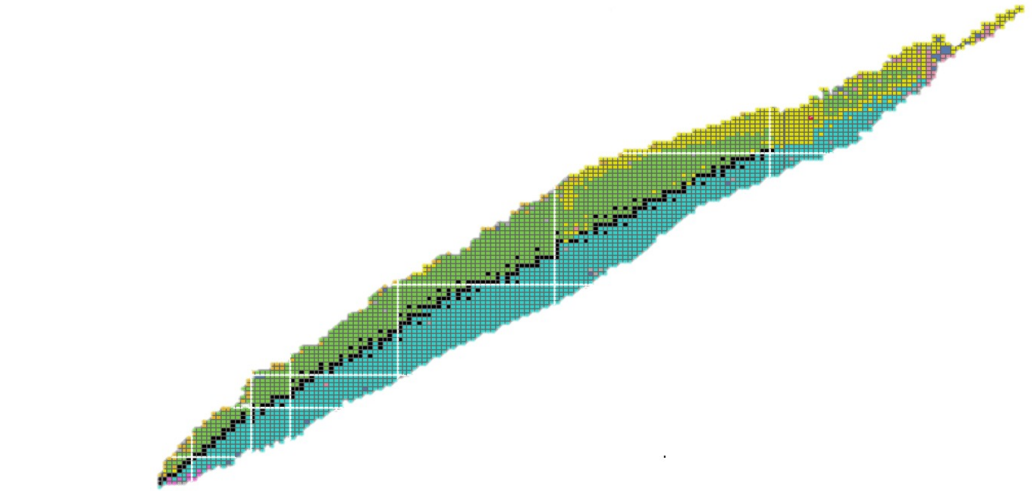

Low energy community

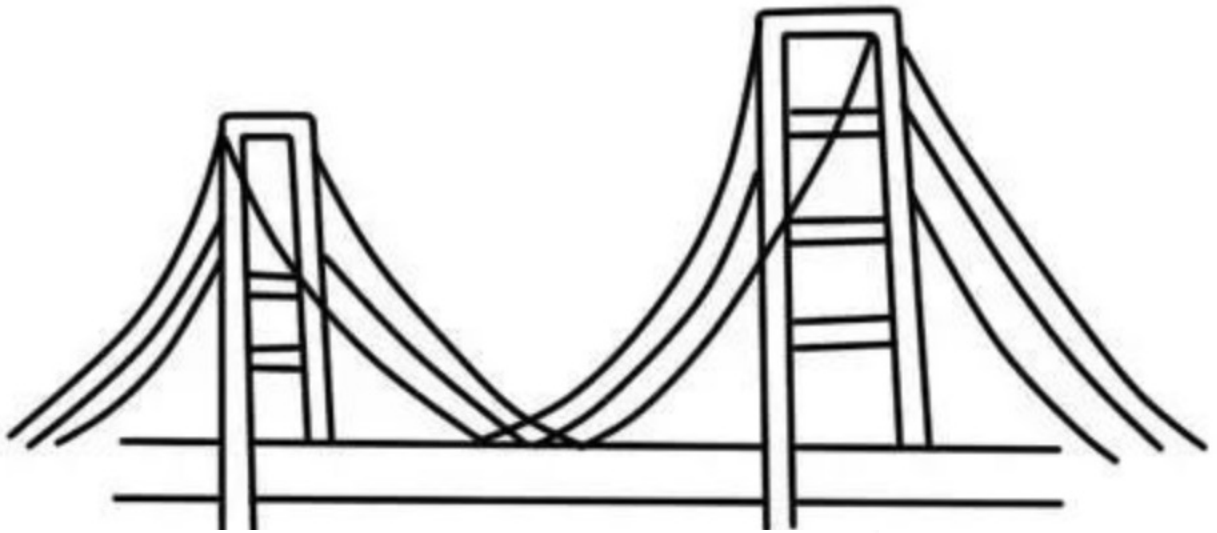

Heavy-ion community

Outline

1. Nuclear structure and heavy-ion collisions

2. Nuclear deformation in large collision system at RHIC and LHC

3. Nuclear structure in isobar collisions at RHIC

4. Future endeavors and opportunities

5. Conclusions and outlooks

Nuclear deformation, neutron skin, and nucleonic clustering

A. Trzcinska et al., PRL 87, 082501(2001) M. Centelles et al., PRL 102, 122502(2009)

Quadrupole

$1 + \beta_2 Y_{2,0}(\theta, \phi)$

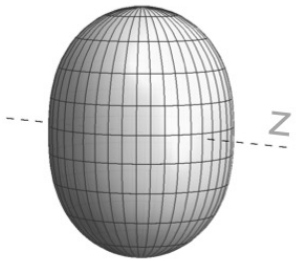

Octupole (pear-shaped) deformation

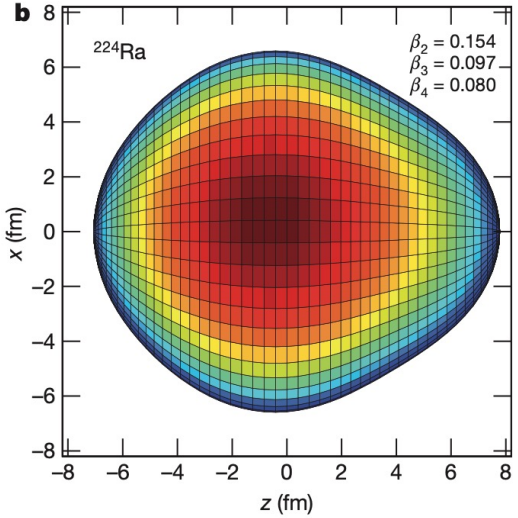

L. O. Gaffney et al., Nature 497, 199 (2013)

Neutron skin $\Delta r_{np} = \langle r_n^2 \rangle^{1/2} - \langle r_p^2 \rangle^{1/2}$

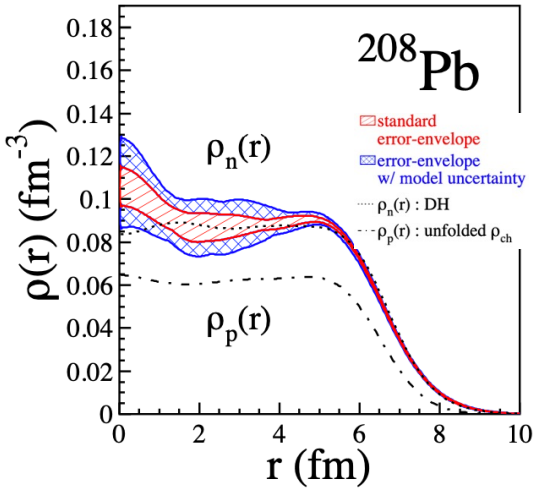

Symmetry energy

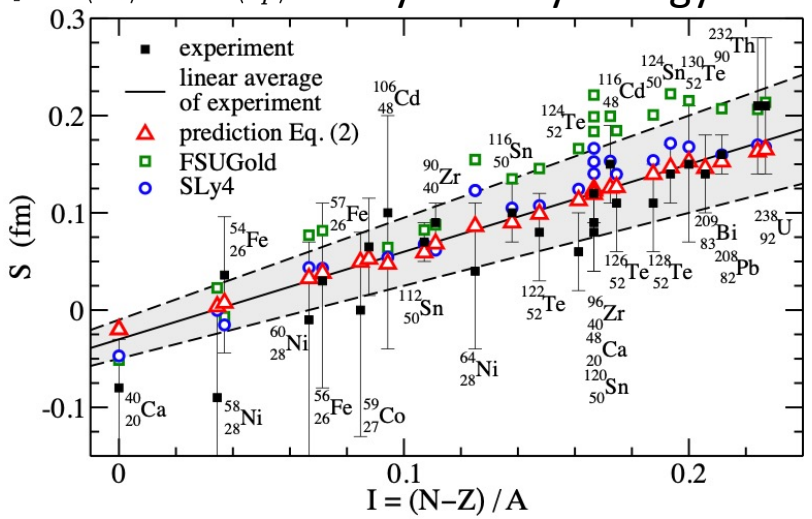

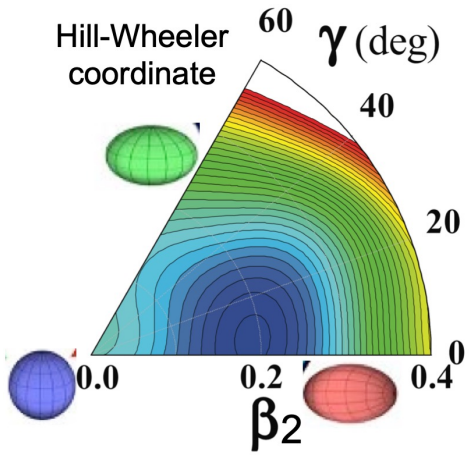

Triaxial spheroid

A. N. Andreyev et al., Nature 405, 430 (2000)

S. Cwiok et al., Nature 433, 705(2005)

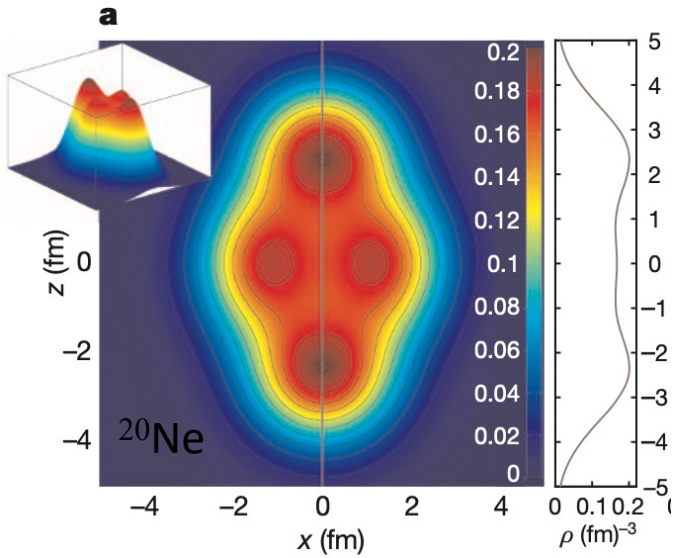

nucleonic clustering in light nuclei

J.P. Ebran et al., Nature 478, 341(2012)

Unique RHIC and LHC runs

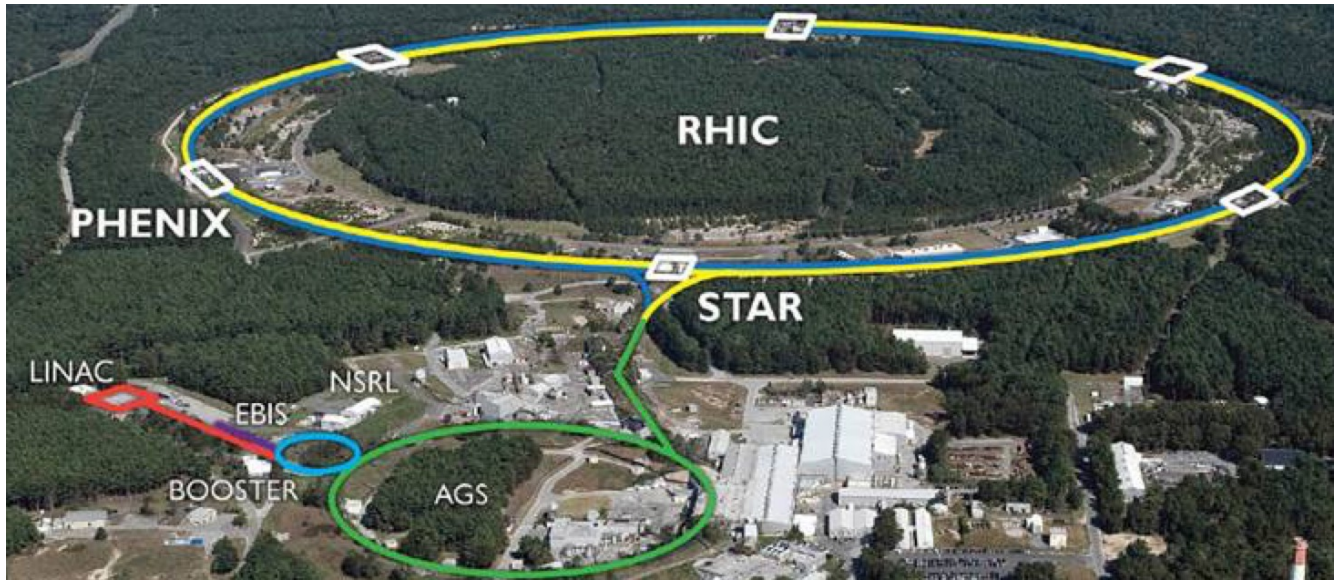

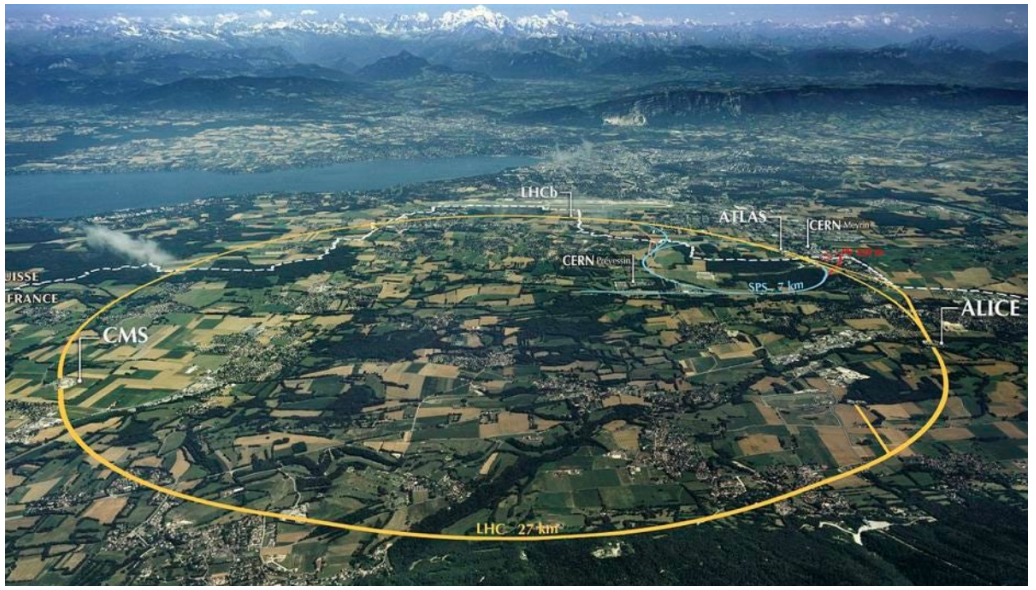

RHIC energies, species combinations and luminosities (Run-1 to 22)

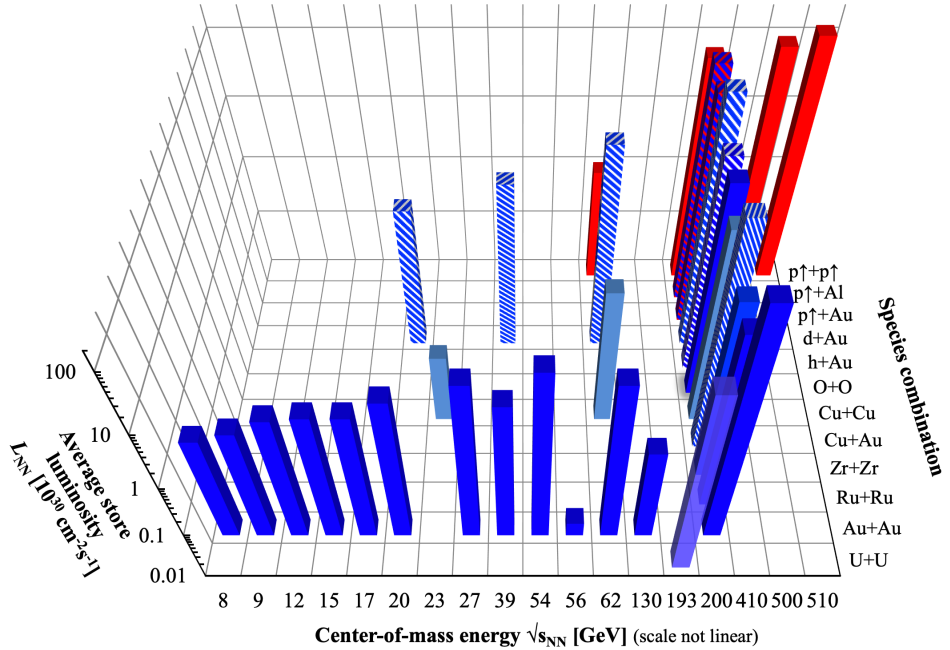

12 one-month heavy-ion runs between 2010 and 2030. **6/12 done**.

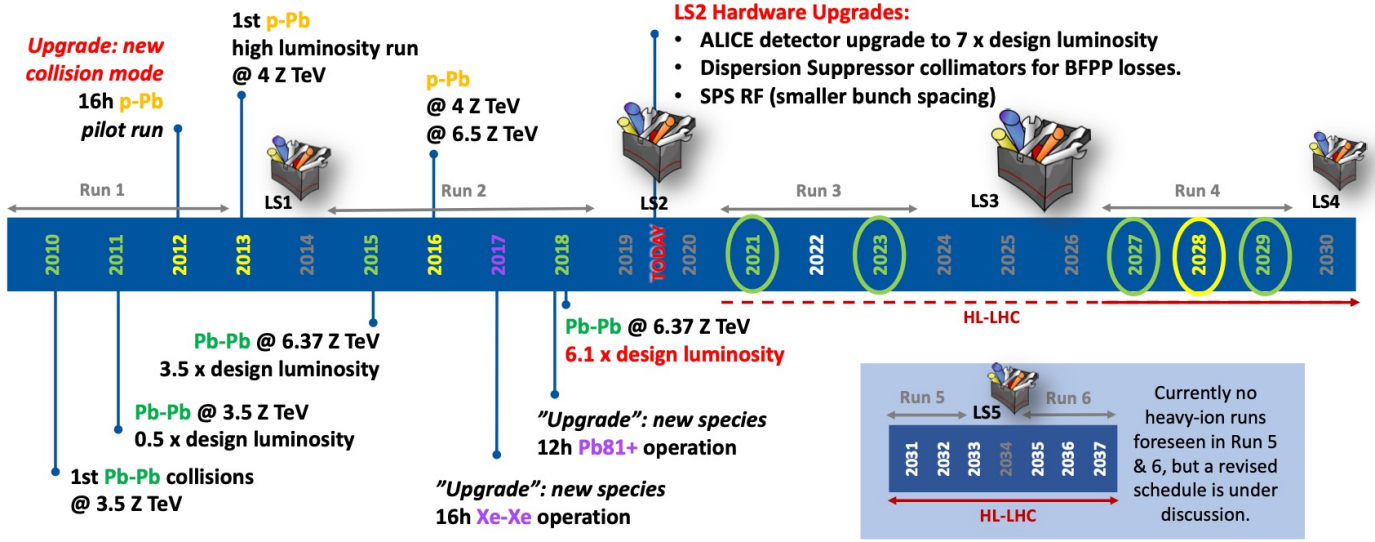

Relativistic heavy-ion collisions

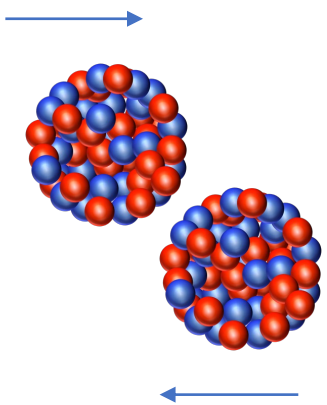

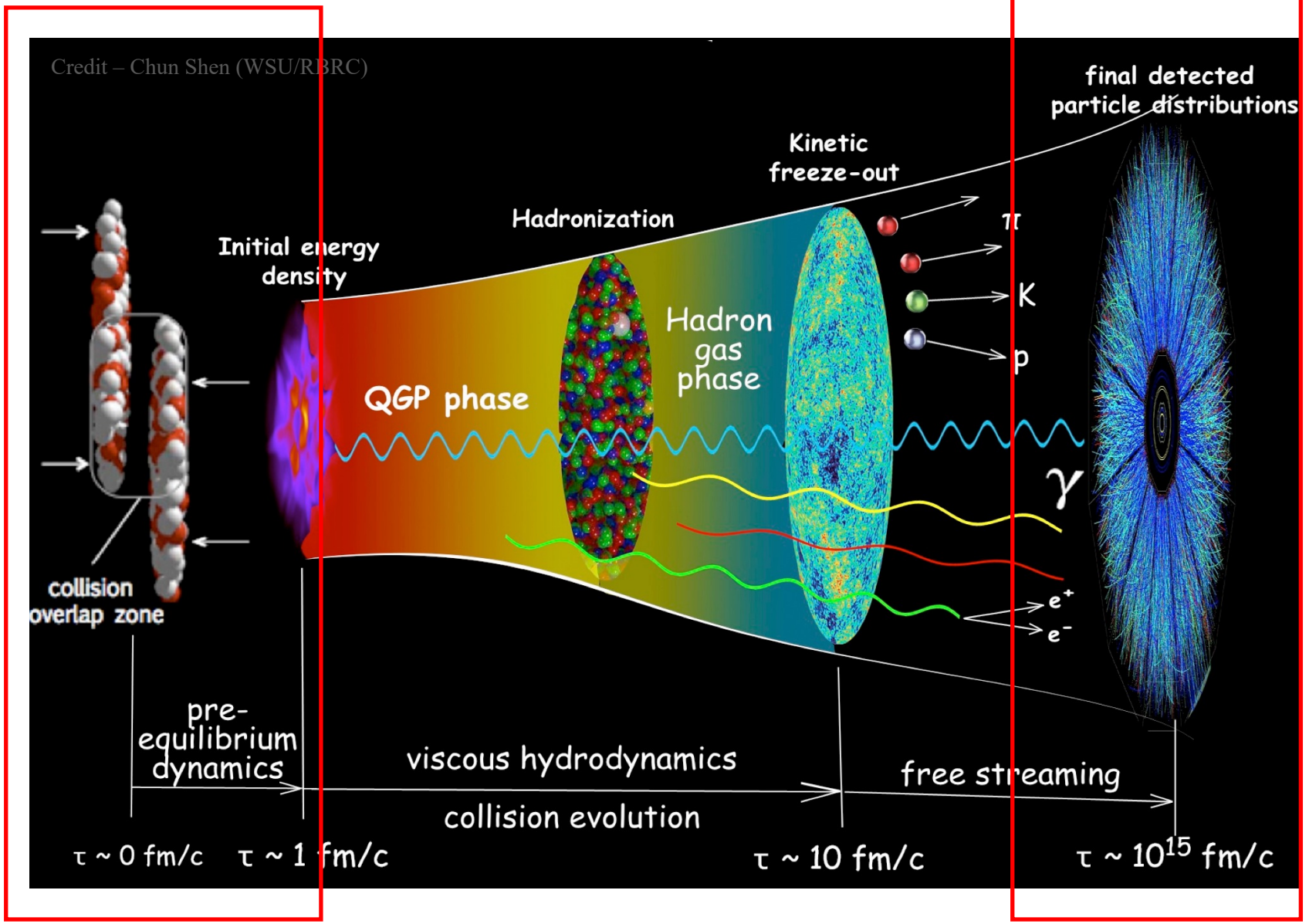

Multiple stage /Complex dynamics

Hybrid multi-stage Modeling with event-by -event fluctuations

Hydrodynamic response to initial state

Nuclear Structure

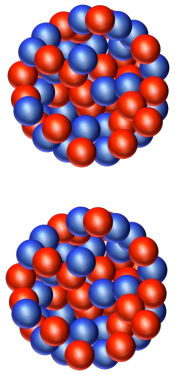

$$\rho(r,\theta,\phi) = \frac{\rho_0}{1+e^{(r-R(\theta,\phi))/a_0}}$$

$$R(\theta,\phi) = R_0(1+\beta_2[\cos\gamma Y_{2,0}(\theta,\phi) + \sin\gamma Y_{2,2}(\theta,\phi)] + \beta_3 Y_{3,0}(\theta,\phi))$$

Imaging?

Initial State

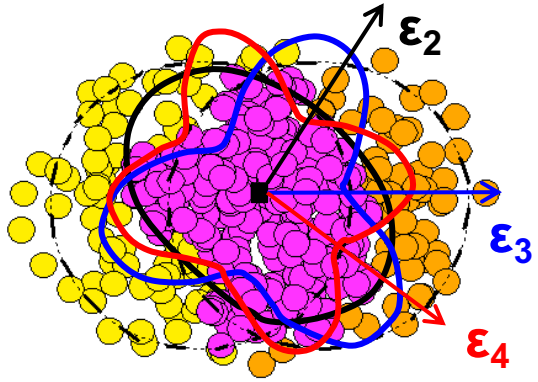

hydrodynamic response

Approximate linear response in each event:

D. Teaney and L. Yan, PRC86, 044908 (2012)

Produced Particle Flow

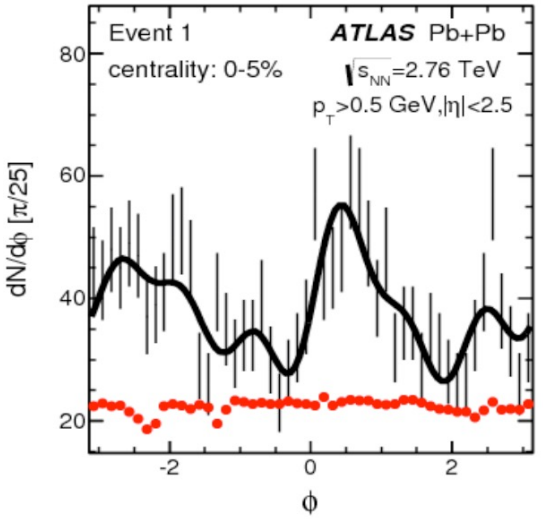

Radial Flow Anisotropic Flow

$$\frac{d^2N}{d\phi dp_T} = N(p_T)\left(\sum_n V_n e^{-in\phi}\right)$$

Initial Size

$$R_\perp^2 \propto \langle r_\perp^2 \rangle$$

Initial Shape

$$\mathcal{E}_n \propto \langle r_\perp^n e^{in\phi} \rangle$$

?

R_0 a_0 β_n

- β_2 → Quadrupole deformation
- β_3 → Octupole deformation
- γ → Triaxiality
- a_0 → Surface diffuseness
- R_0 → Nuclear size

High energy: approximate linear response in each event

$$N_{ch} \propto N_{part} \quad \frac{\delta[p_T]}{[p_T]} \propto -\frac{\delta R_\perp}{R_\perp} \quad V_n \propto \mathcal{E}_n$$

Nuclear deformation in ^{238}U at RHIC and ^{129}Xe at LHC

$$\rho(r,\theta,\phi) = \frac{\rho_0}{1+e^{(r-R(\theta,\phi))/a_0}}$$

$$R(\theta,\phi) = R_0(1+\beta_2[\cos\gamma Y_{2,0}(\theta,\phi) + \sin\gamma Y_{2,2}(\theta,\phi)] + \beta_3 Y_{3,0}(\theta,\phi) + \beta_4 Y_{4,0}(\theta,\phi))$$

Role of nuclear deformation in the initial state

Jia, PRC105, 014905(2021), PRC105, 044905(2021)

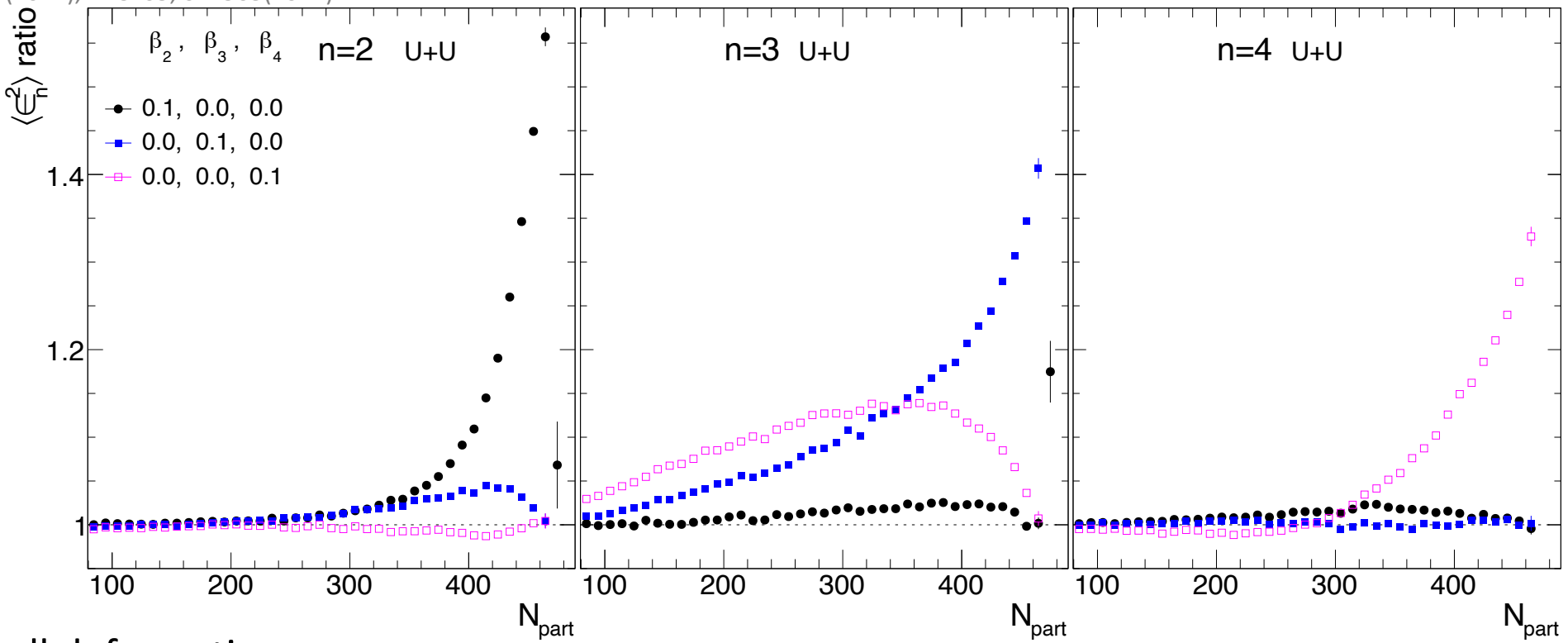

For small deformations:

$$\langle \varepsilon_n^2 \rangle = a_n + \sum b_{n,m}\beta_m^2$$

Glauber model shows:

$$\langle \varepsilon_2^2 \rangle \approx a_2 + b_{2,2}\beta_2^2 + b_{2,3}\beta_3^2$$
$$\langle \varepsilon_3^2 \rangle \approx a_3 + b_{3,3}\beta_3^2 + b_{3,4}\beta_4^2$$
$$\langle \varepsilon_4^2 \rangle \approx a_4 + b_{4,4}\beta_4^2$$

Assume linear response: $\langle v_n^2 \rangle \propto \langle \varepsilon_n^2 \rangle$

Expected behavior for final state flow:

$$\langle v_2^2 \rangle \approx a_2 + b_{2,2}\beta_2^2 + b_{2,3}\beta_3^2$$
$$\langle v_3^2 \rangle \approx a_3 + b_{3,3}\beta_3^2 + b_{3,4}\beta_4^2$$
$$\langle v_4^2 \rangle \approx a_4 + b_{4,4}\beta_4^2$$

← Valid only in central region

9

Role of nuclear deformation in the initial state

Jia, PRC105, 014905(2021), PRC105, 044905(2021)

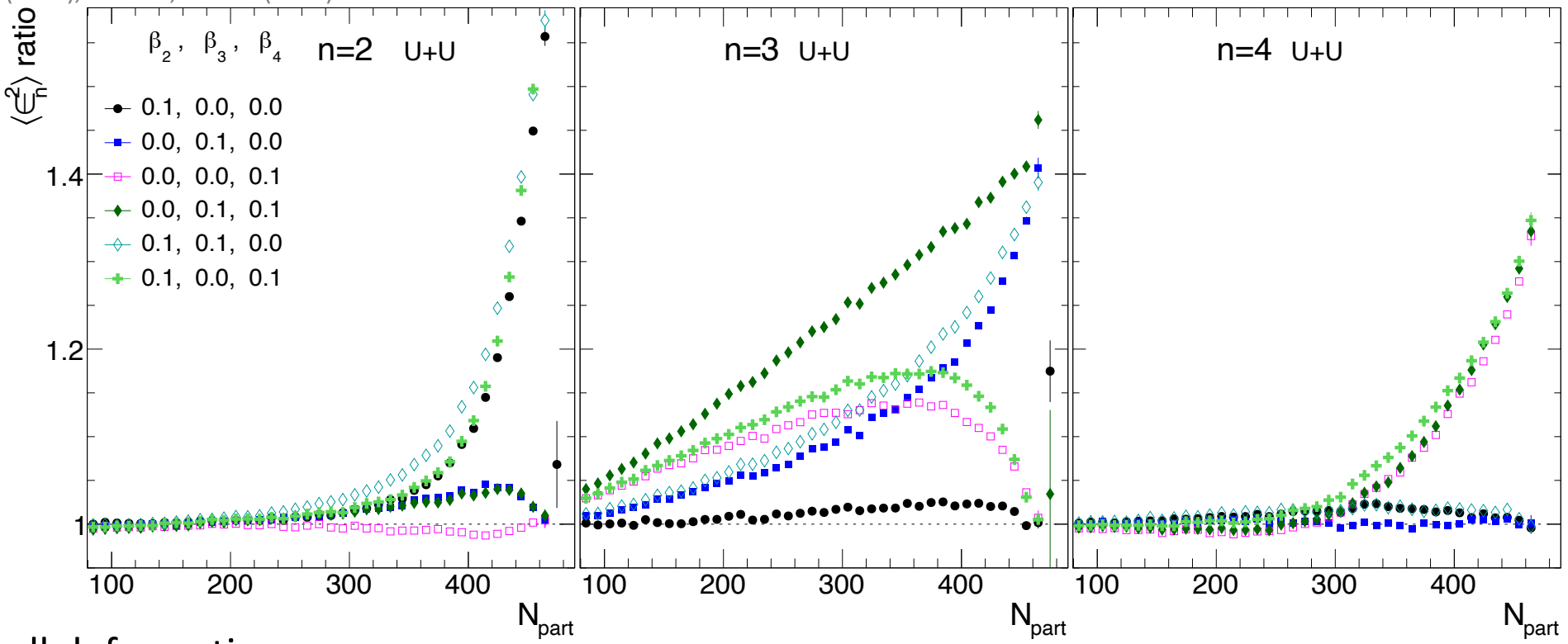

For small deformations:

$$\langle \varepsilon_n^2 \rangle = a_n + \sum b_{n,m}\beta_m^2$$

Glauber model shows:

$$\langle \varepsilon_2^2 \rangle \approx a_2 + b_{2,2}\beta_2^2 + b_{2,3}\beta_3^2$$
$$\langle \varepsilon_3^2 \rangle \approx a_3 + b_{3,3}\beta_3^2 + b_{3,4}\beta_4^2$$
$$\langle \varepsilon_4^2 \rangle \approx a_4 + b_{4,4}\beta_4^2$$

Assume linear response: $\langle v_n^2 \rangle \propto \langle \varepsilon_n^2 \rangle$

Expected behavior for final state flow:

$$\langle v_2^2 \rangle \approx a_2 + b_{2,2}\beta_2^2 + b_{2,3}\beta_3^2$$
$$\langle v_3^2 \rangle \approx a_3 + b_{3,3}\beta_3^2 + b_{3,4}\beta_4^2$$
$$\langle v_4^2 \rangle \approx a_4 + b_{4,4}\beta_4^2$$

← Valid only in central region

Role of nuclear deformation in the initial state

Jia, PRC105, 014905(2021), PRC105, 044905(2021)

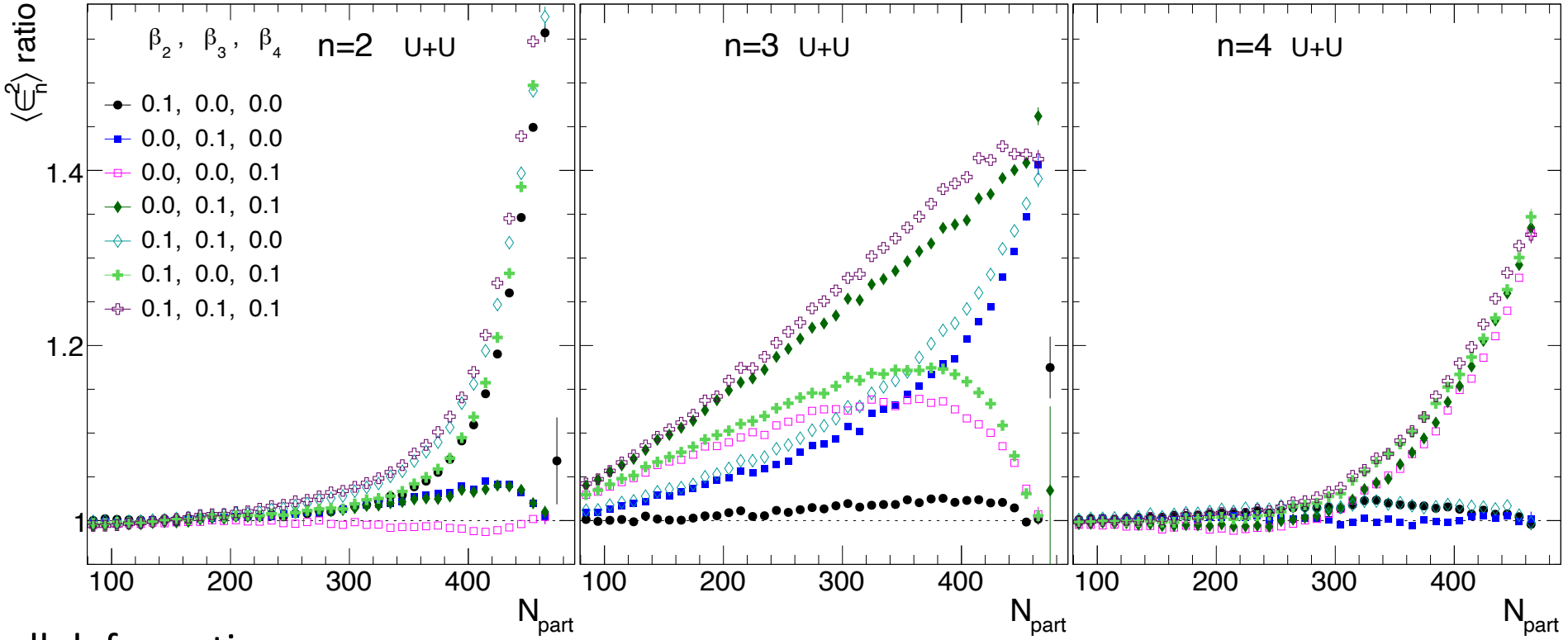

For small deformations:

$$\langle \varepsilon_n^2 \rangle = a_n + \sum b_{n,m} \beta_m^2$$

Glauber model shows:

$$\langle \varepsilon_2^2 \rangle \approx a_2 + b_{2,2}\beta_2^2 + b_{2,3}\beta_3^2$$
$$\langle \varepsilon_3^2 \rangle \approx a_3 + b_{3,3}\beta_3^2 + b_{3,4}\beta_4^2$$
$$\langle \varepsilon_4^2 \rangle \approx a_4 + b_{4,4}\beta_4^2$$

Assume linear response: $\langle v_n^2 \rangle \propto \langle \varepsilon_n^2 \rangle$

Expected behavior for final state flow:

$$\langle v_2^2 \rangle \approx a_2 + b_{2,2}\beta_2^2 + b_{2,3}\beta_3^2$$
$$\langle v_3^2 \rangle \approx a_3 + b_{3,3}\beta_3^2 + b_{3,4}\beta_4^2$$
$$\langle v_4^2 \rangle \approx a_4 + b_{4,4}\beta_4^2$$

← Valid only in central region

Role of nuclear deformation in the final state

G. Giacalone, J. Jia and C. Zhang, PRL127, 242301 (2021)

Also see, STAR, PRL 115, 222301 (2015)

Final state implemented in AMPT transport model

Only is β_2 effects are studied
Nice linear relation observed

$$\langle v_2^2 \rangle \approx a_2 + b_{2,2}\beta_2^2$$

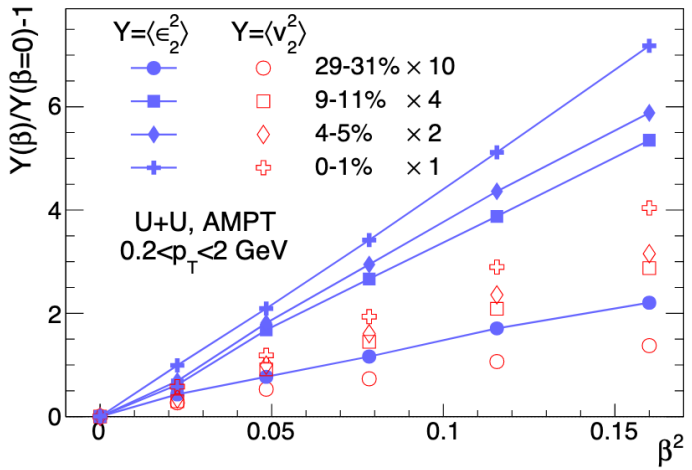

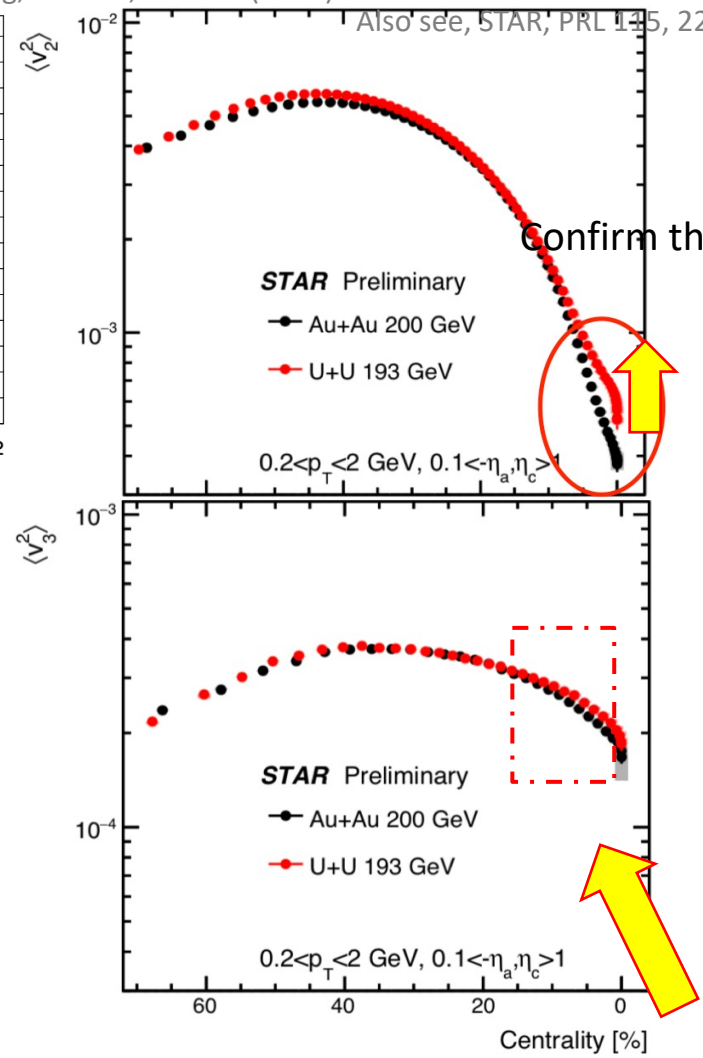

Confirm the role of β_2

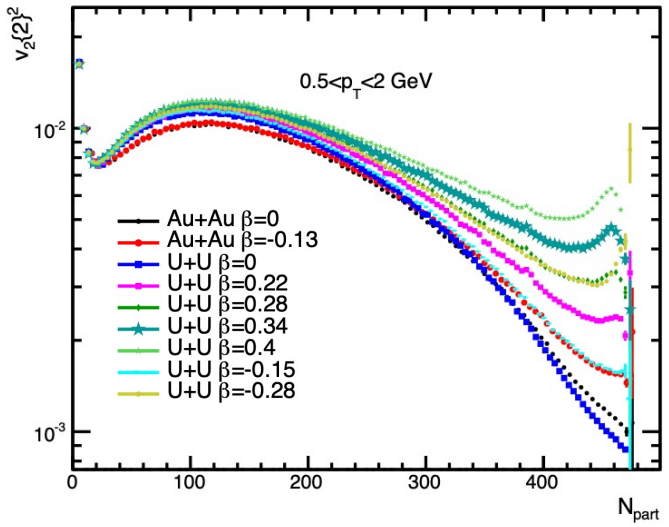

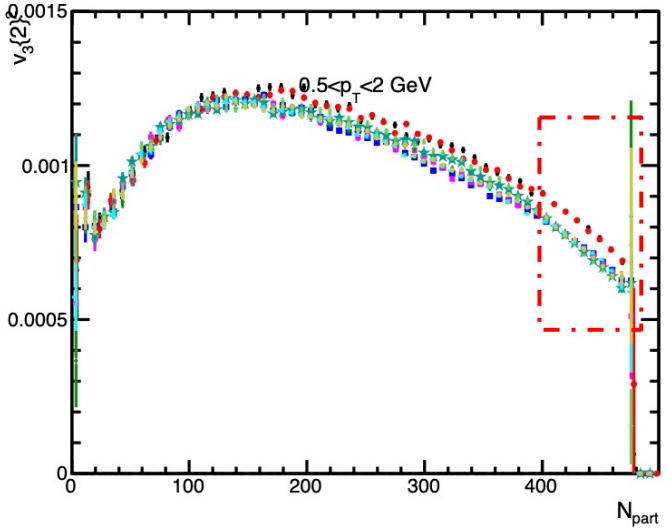

v_3 is fluctuation driven, expect in central $\langle v_3^2 \rangle \propto \langle \varepsilon_3^2 \rangle \sim 1/A$

i.e. $v_{3,U} < v_{3,Au}$ in absence of β_3 and β_4 (A: Mass number)

But STAR v_3 data show reversed ordering in central

Role of nuclear deformation in the final state

We plot ratio of v_n in AuAu with β_2=-0.13 to UU with different $(\beta_2, \beta_3, \beta_4)$

β_2	β_3	β_4
$0.286[12]$	$0.078[13]$	$0.07-0.09[14,15]$

S. E. Agbemava et al., PRC 93, 044304 (2016)

J. Libert et al., PRC 25, 586 (1982)

P. Moller et al., ADNDT 109-110, 1 (2016)

Confirms:

$$\langle v_2^2 \rangle \approx a_2 + b_{2,2}\beta_2^2 + b_{2,3}\beta_3^2$$
$$\langle v_3^2 \rangle \approx a_3 + b_{3,3}\beta_3^2 + b_{3,4}\beta_4^2$$
$$\langle v_4^2 \rangle \approx a_4 + b_{4,4}\beta_4^2$$

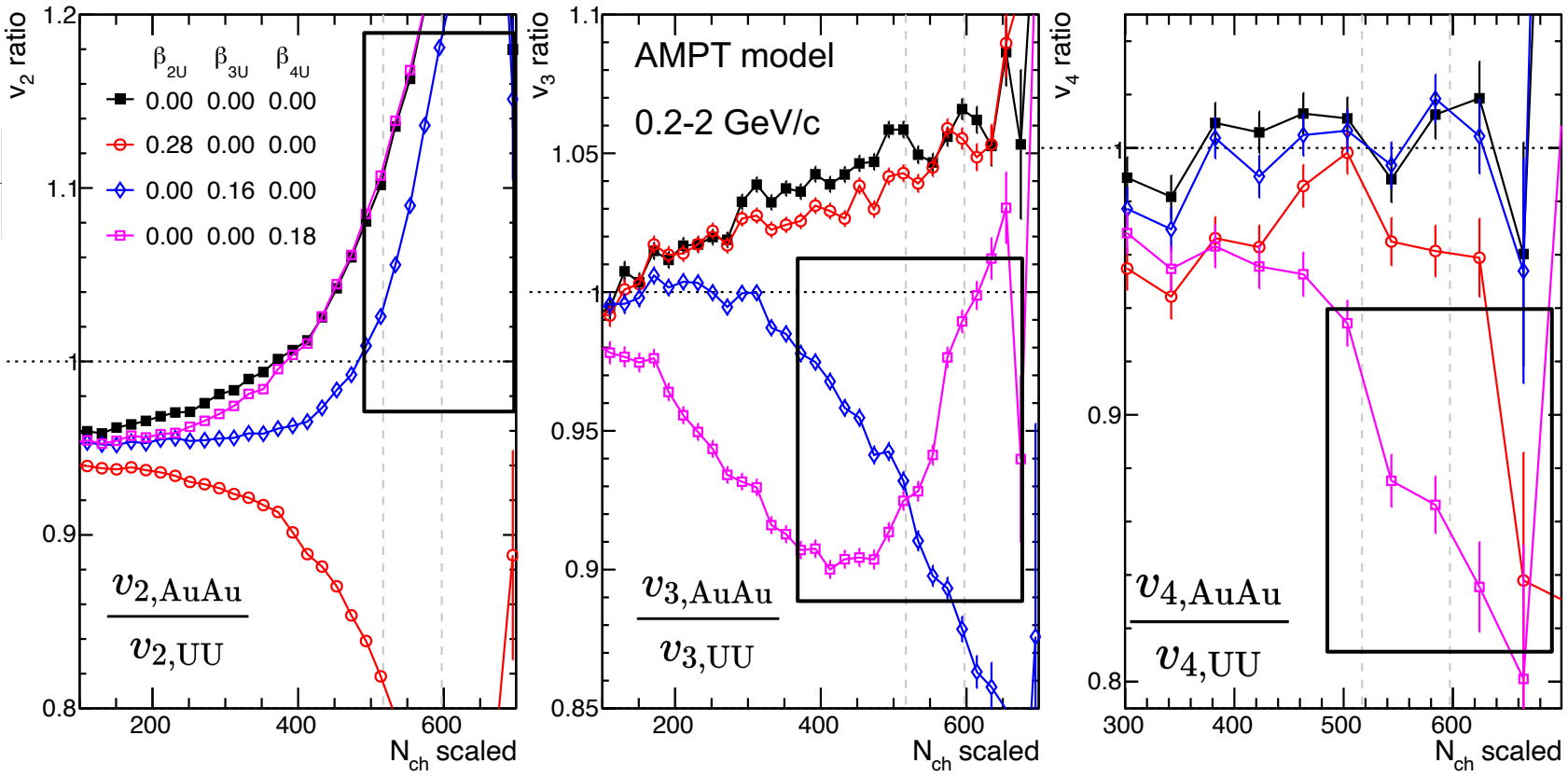

$\beta_{4,U}$ constrained using v_4 ratio in the central region

v_2 ratio is mostly affected by $\beta_{2,U}$, but also $\beta_{3,U}$

Order of v_3 reversed by considering non-zero $\beta_{3,U}, \beta_{4,U}$ which can be constrained in the central region.

Indication of the octupole and hexadecapole in ^{238}U nuclei in heavy ion collisions

Role of nuclear deformation in the final state

We plot ratio of v_n in AuAu with β_2=-0.13 to UU with different $(\beta_2, \beta_3, \beta_4)$

β_2	β_3	β_4
$0.286[12]$	$0.078[13]$	$0.07-0.09[14,15]$

S. E. Agbemava et al., PRC 93, 044304 (2016)

J. Libert et al., PRC 25, 586 (1982)

P. Moller et al., ADNDT 109-110, 1 (2016)

Confirms:

$$\langle v_2^2 \rangle \approx a_2 + b_{2,2}\beta_2^2 + b_{2,3}\beta_3^2$$
$$\langle v_3^2 \rangle \approx a_3 + b_{3,3}\beta_3^2 + b_{3,4}\beta_4^2$$
$$\langle v_4^2 \rangle \approx a_4 + b_{4,4}\beta_4^2$$

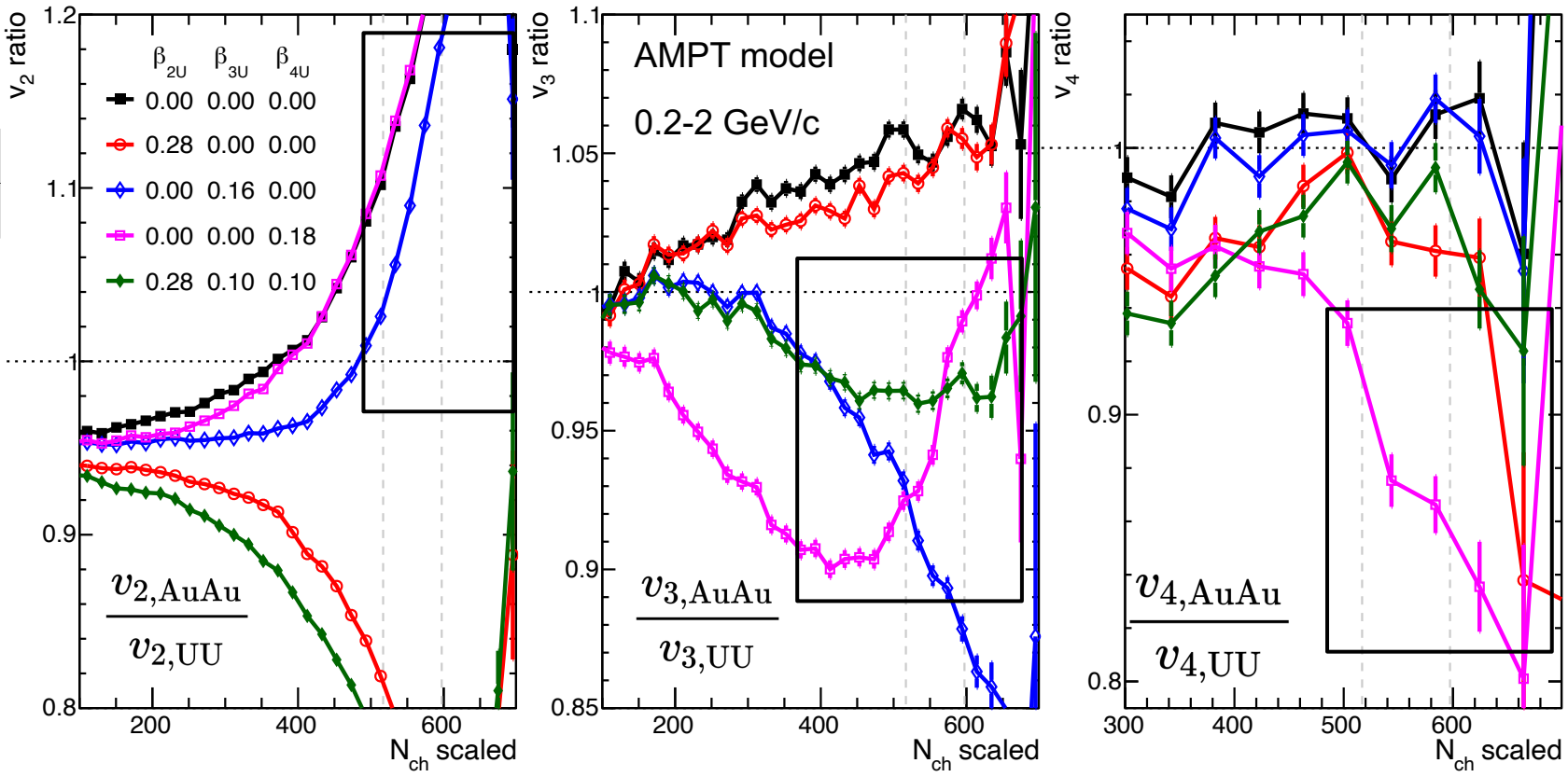

$\beta_{4,U}$ constrained using v_4 ratio in the central region

v_2 ratio is mostly affected by $\beta_{2,U}$, but also $\beta_{3,U}$

Order of v_3 reversed by considering non-zero $\beta_{3,U}, \beta_{4,U}$ which can be constrained in the central region.

Indication of the octupole and hexadecapole in ^{238}U nuclei in heavy ion collisions

[p_T] fluctuations

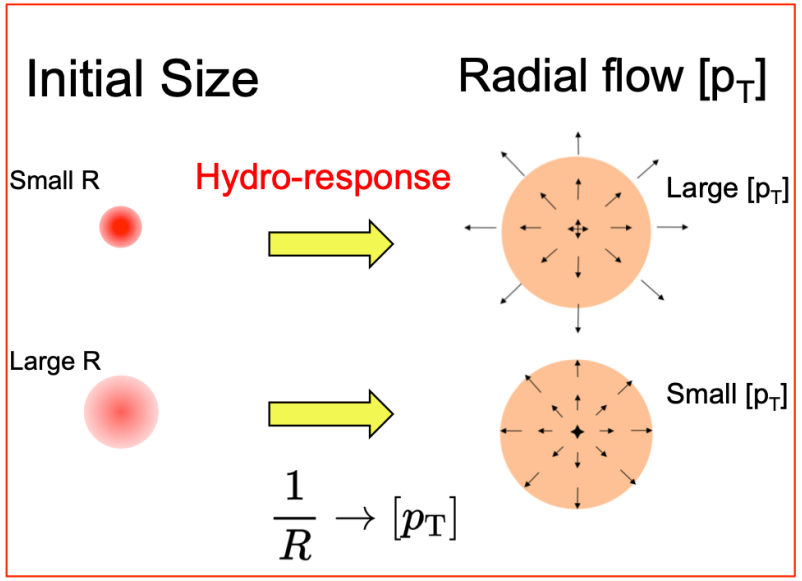

J. Jia, PRC 105, 044905 (2021)

Mean $\frac{\delta[p_T]}{[p_T]} \propto \frac{\delta d_\perp}{d_\perp} \propto \beta_2$

Variance $\left\langle \left(\frac{\delta[p_T]}{[p_T]}\right)^2 \right\rangle \propto \left\langle \left(\frac{\delta d_\perp}{d_\perp}\right)^2 \right\rangle \propto \beta_2^2$

Skewness $\left\langle \left(\frac{\delta[p_T]}{[p_T]}\right)^3 \right\rangle \propto \left\langle \left(\frac{\delta d_\perp}{d_\perp}\right)^3 \right\rangle \propto cos(3\gamma)\beta_2^3$

Kurtosis $\left\langle \left(\frac{\delta[p_T]}{[p_T]}\right)^4 \right\rangle - 3\left\langle \left(\frac{\delta[p_T]}{[p_T]}\right)^2 \right\rangle^2 \propto \left\langle \left(\frac{\delta d_\perp}{d_\perp}\right)^4 \right\rangle - 3\left\langle \left(\frac{\delta d_\perp}{d_\perp}\right)^2 \right\rangle^2 \propto -\beta_2^4$

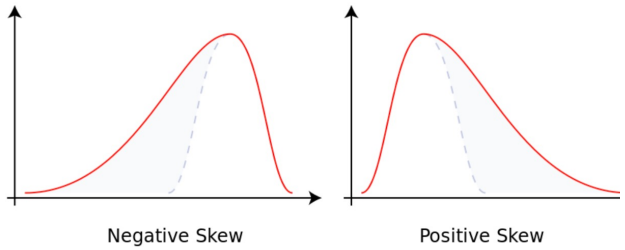

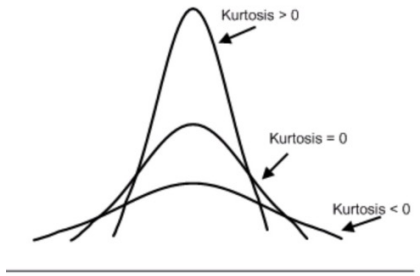

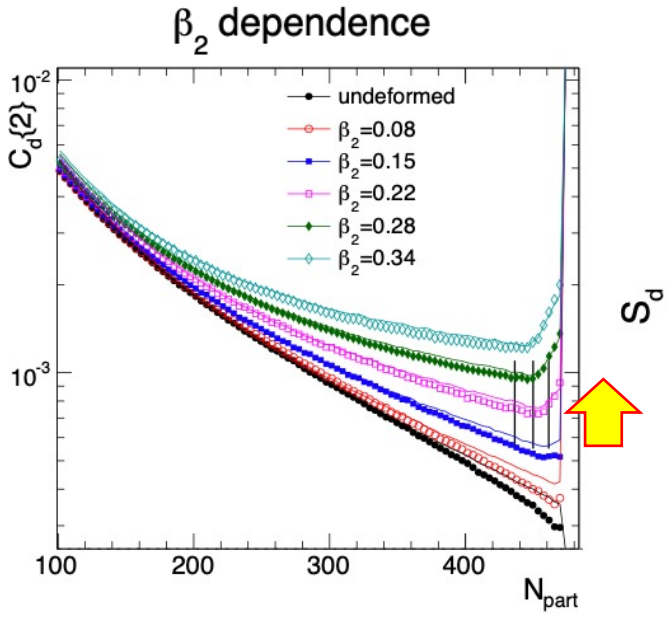

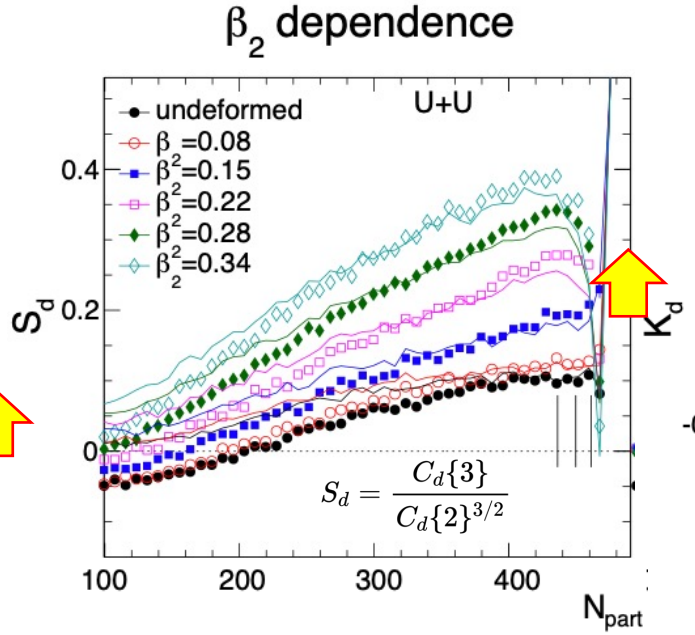

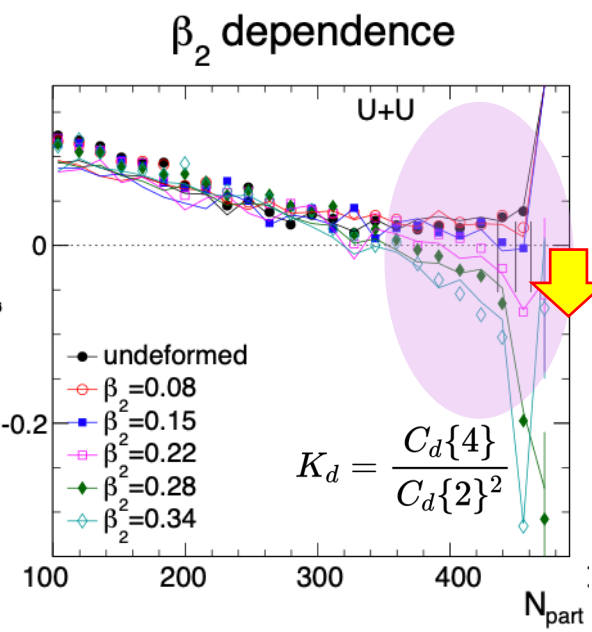

[p_T] fluctuations at RHIC and comparisons to CGC+hydro model

IP-Glasma+Hydro: private calculation provided by Bjoern Schenke

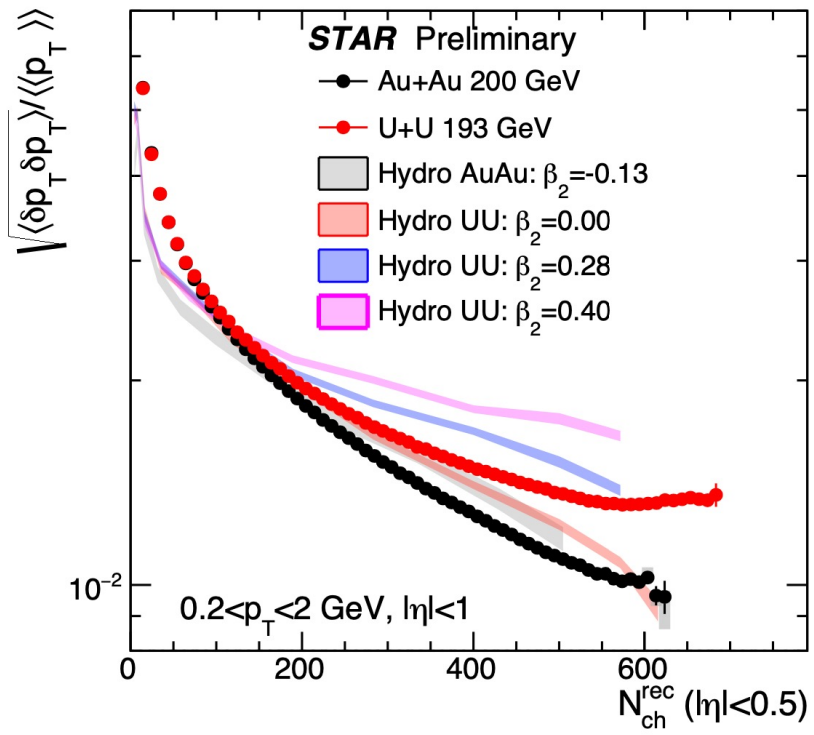

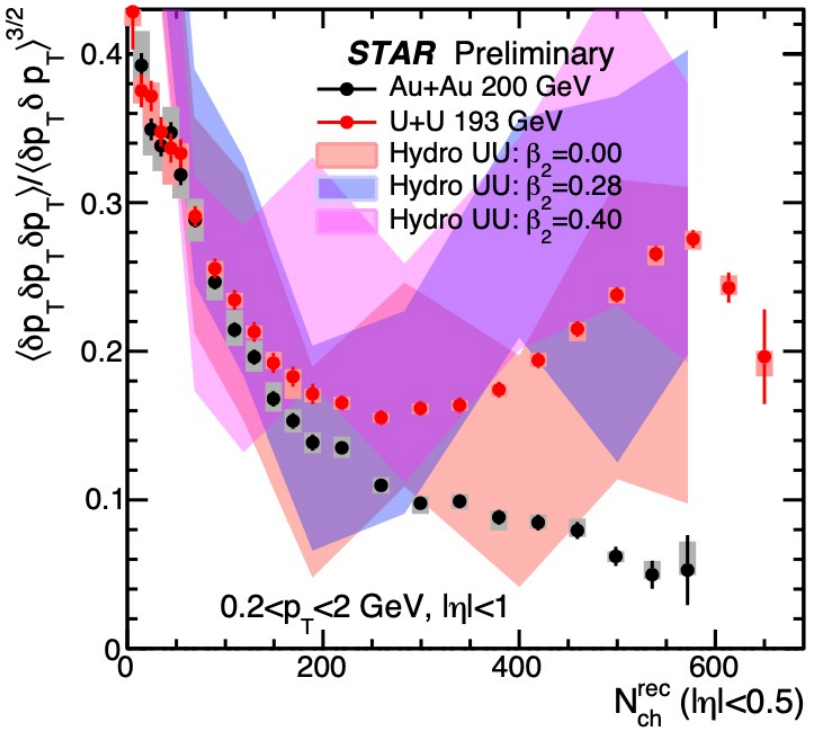

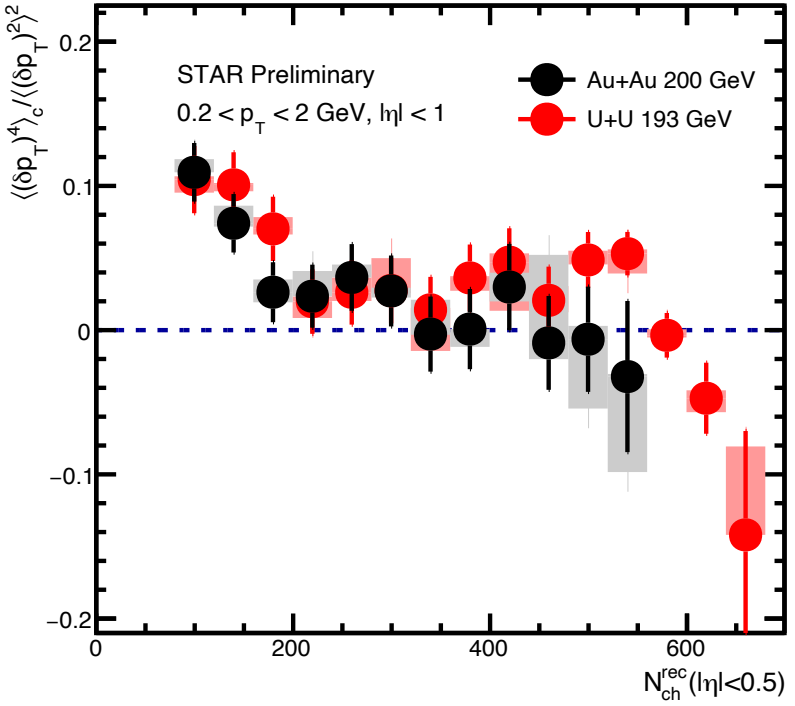

Au+Au: follow independent source scaling 1/N within power-law decrease

U+U: large enhancement in normalized variance and skewness and sign-change in normalized kurtosis

⟶ size fluctuations enhanced

Nuclear deformation role is confirmed by hydro calculations.

Radial expansion induced by nuclei shape:

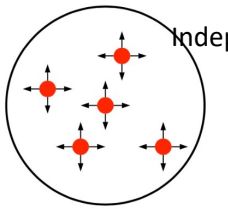

$$c_s^2 = \frac{dP}{d\epsilon} = \frac{d\ln T}{d\ln s} = \frac{d\ln\langle p_T\rangle}{d\ln N_{ch}}$$

$$\frac{d\langle p_t\rangle}{\langle\langle p_t\rangle\rangle} = -3c_s^2\frac{dR}{\langle R\rangle}$$

Collecting the initial state to the nuclear geometry

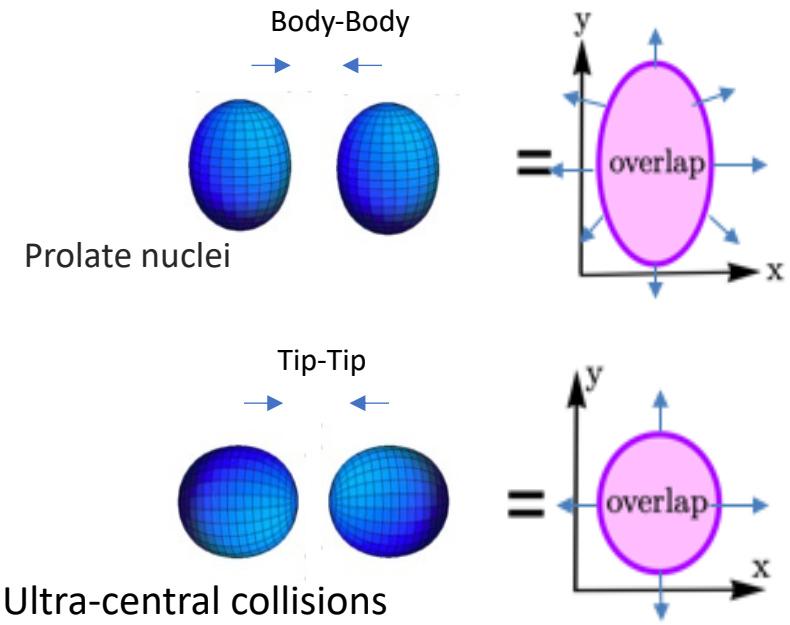

- $\boldsymbol{\varepsilon}_2$ and R are influenced by the quadrupole deformation β_2
- $\langle p_T \rangle \sim 1/R$ and $v_2 \propto \boldsymbol{\varepsilon}_2$: $\left\langle \epsilon_n^2 \frac{1}{R} \right\rangle \rightarrow \langle v_n^2 \, p_T \rangle$

  deformation contributes to anticorrelation between v_2 and $\langle p_T \rangle$

Pearson coefficient: v_n-$[p_T]$ three particle correlator

$$\rho\left(v_n^2, [p_T]\right) = \frac{\mathrm{cov}\left(v_n^2, [p_T]\right)}{\sqrt{\mathrm{Var}\left(v_n^2\right)_{\mathrm{dyn}} \langle \delta p_T \delta p_T \rangle}}$$

$$\mathrm{cov}\left(v_n^2, [p_T]\right) \equiv \left\langle \frac{\sum_{i \neq j \neq k} w_i w_j w_k e^{in\phi_i} e^{-in\phi_j} (p_{T,k} - \langle\langle p_T \rangle\rangle)}{\sum_{i \neq j \neq k} w_i w_j w_k} \right\rangle_{\mathrm{evt}}$$

$$[p_T] \equiv \frac{\sum_i w_i p_{T,i}}{\sum_i w_i}, \langle\langle p_T \rangle\rangle \equiv \langle [p_T] \rangle_{\mathrm{evt}}$$

w_i is track weight

$$\mathrm{Var}\left(v_n^2\right)_{\mathrm{dyn}} = v_n\{2\}^4 - v_n\{4\}^4$$

$$\langle \delta p_T \delta p_T \rangle = \left\langle \frac{\sum_{i \neq j} w_i w_j (p_{T,i} - \langle\langle p_T \rangle\rangle)(p_{T,j} - \langle\langle p_T \rangle\rangle)}{\sum_{i \neq j} w_i w_j} \right\rangle_{\mathrm{evt}}$$

P. Bozek, PRC 93, 044908 (2016); ATLAS EPJC 79, 985 (2019); B. Schenke et al., PRC 102, 034905 (2020); G.Giacalone, PRC 102, 024901 (2020); PRL 124, 202301(2020)

v_n - [p_T] correlations at RHIC

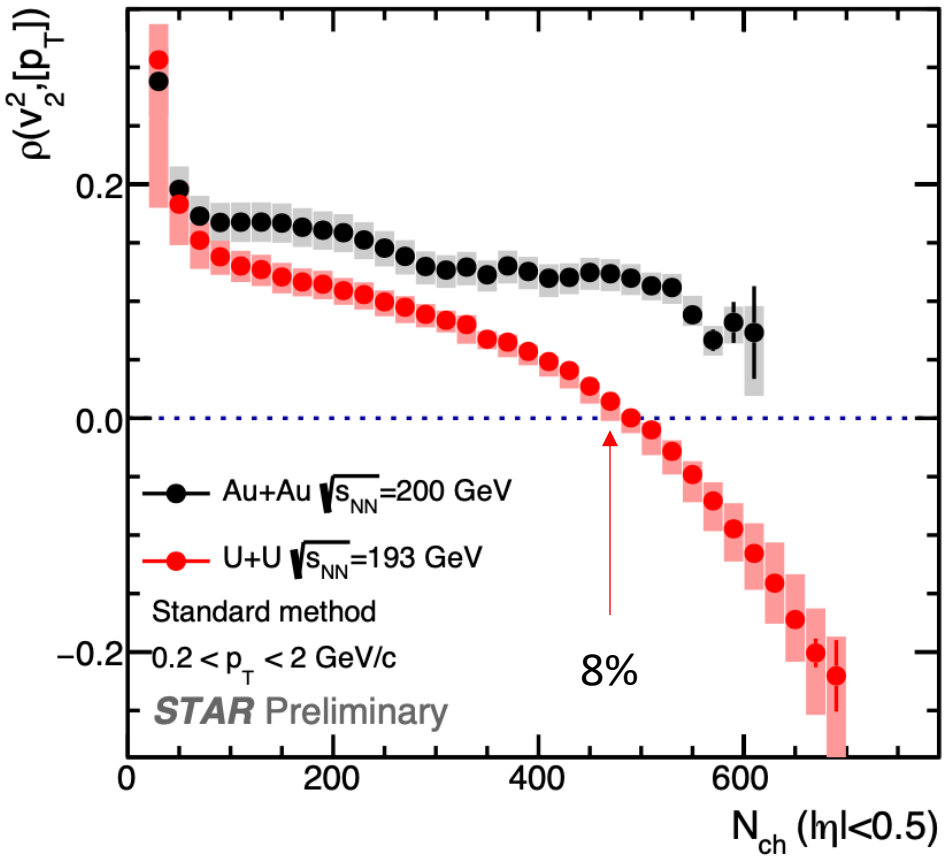

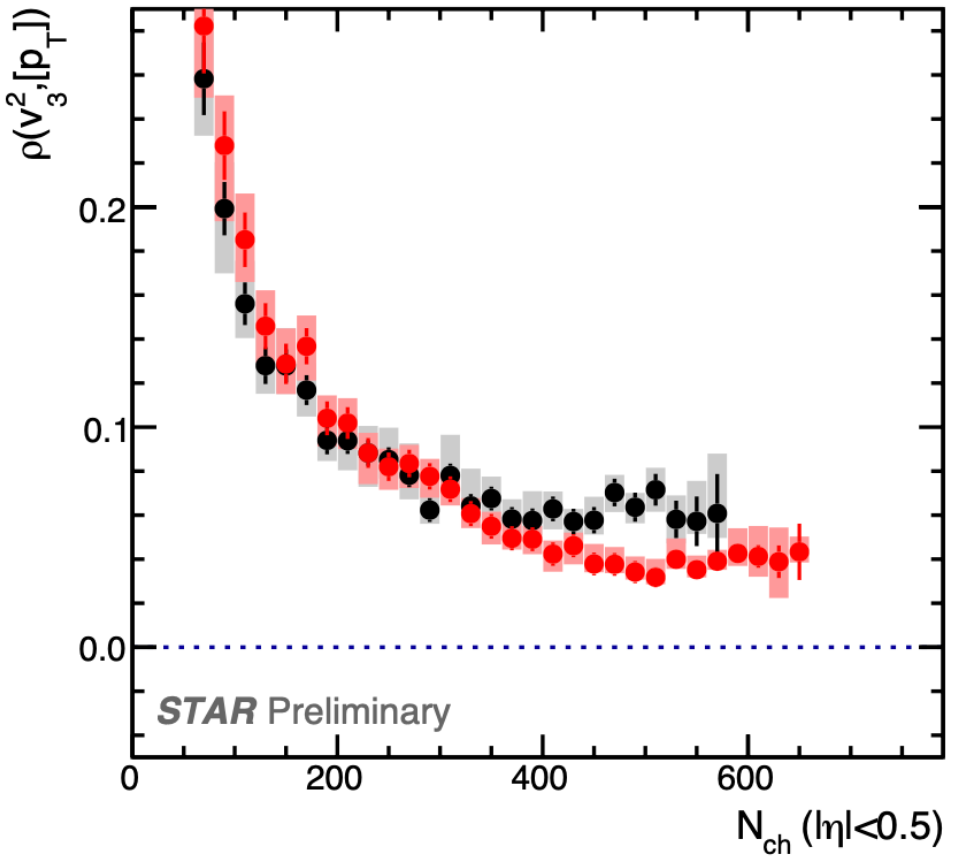

Clear sign change in U+U around 8% centrality
Au+Au remains positive

Similar between Au+Au and U+U

Compare to TRENTo initial-state model

TRENTo provided by Giuliano Giacalone (PRC102, 024901(2020), PRL124, 202301(2020))

Calculated via predictor with assumption: $v_n \propto \epsilon_n$, $[p_T] \propto \frac{E}{S}$

$$\rho(v_n^2, [p_T]) \sim \frac{\langle \epsilon_n^2 \delta \frac{E}{S} \rangle}{\sqrt{\mathrm{var}(\epsilon_n^2) \langle \delta \frac{E}{S} \delta \frac{E}{S} \rangle}}$$

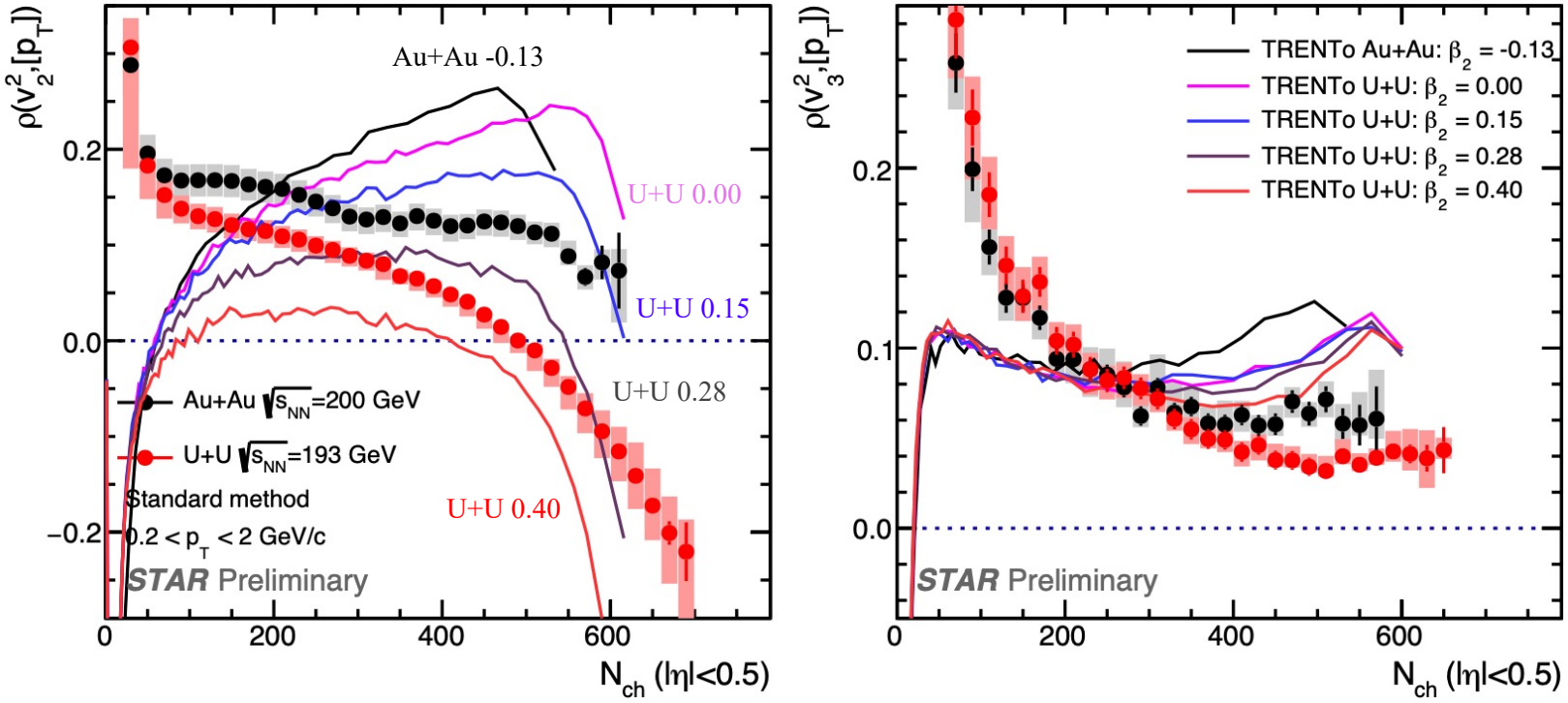

- Trento does not describe data but shows a hierarchical β_2 dependence for correlations
- Trento shows sign-change from Uranium deformation, prefers 0.28< β_2 <0.4
- Trento shows that v_3^2-$[p_T]$ correlations are insensitive to deformation.

Compare to (boost-invariant) CGC+Hydro model

IP-Glasma+Hydro provided by Bjoern Schenke (PRC102, 044905(2020))

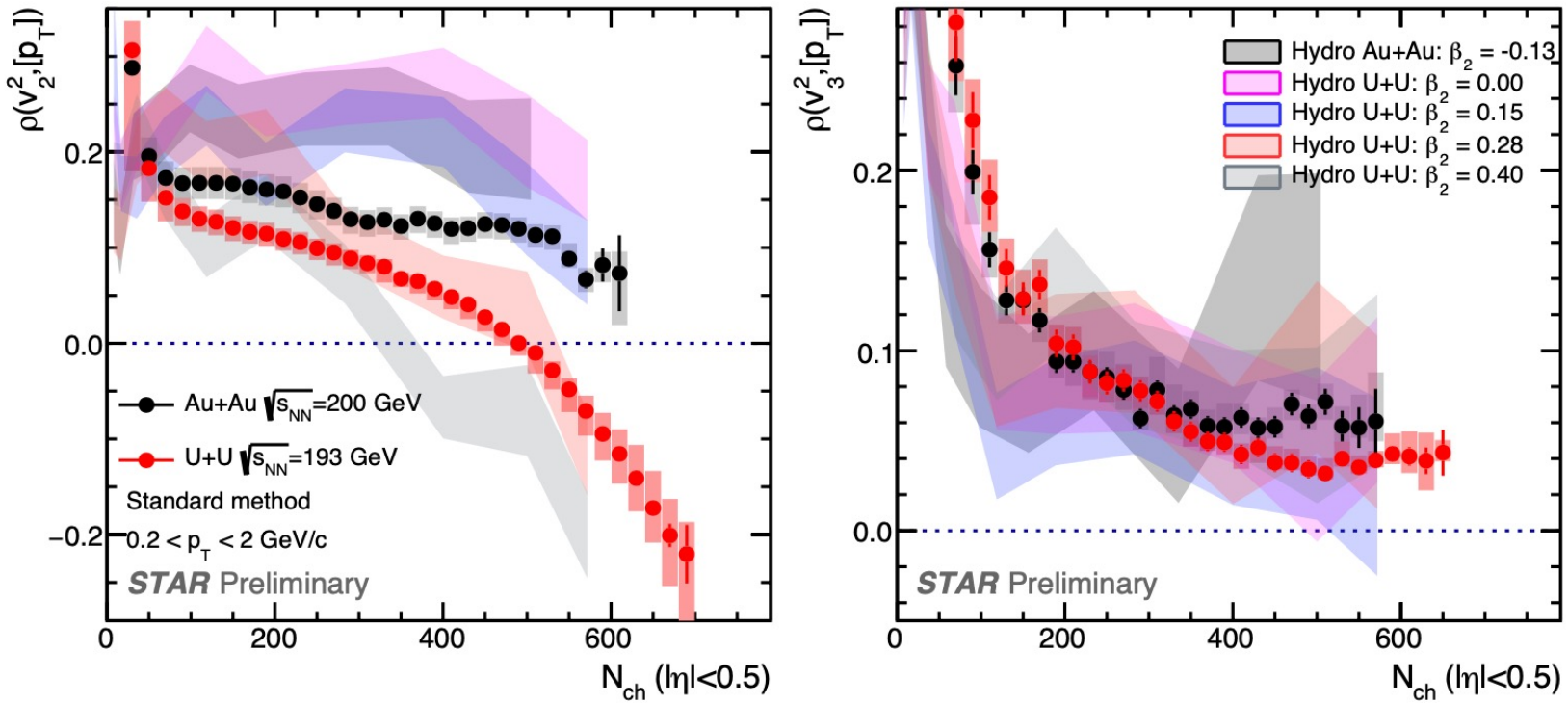

- Without deformation, CGC+hydro model over-predicts the values for $\rho(\mathrm{v}_2^2, [\mathrm{p_T}])$.
- With increasing β_2, model could describe the trend of $\rho(\mathrm{v}_2^2, [\mathrm{p_T}])$.
- Model shows that $\rho(\mathrm{v}_3^2, [\mathrm{p_T}])$ are insensitive to β_2.

The sign-change of $\rho(\mathrm{v}_2^2, [\mathrm{p_T}])$ is due to deformation effect, model quantifies the β_2 value around 0.3 with large uncertainty.

Evidence of the quadrupole and triaxial structure of ^{129}Xe at LHC

Triaxial

J. Jia, PRC105, 044905(2021)

$\beta_2 = 0.25, \cos(3\gamma) = 0$

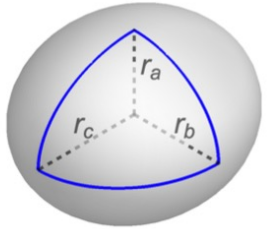

$r_a \neq r_b \neq r_c$

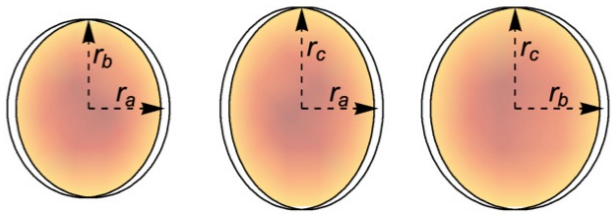

$$\rho(r,\theta,\phi) = \frac{\rho_0}{1 + e^{[r - R(\theta,\phi)/a_0]}}$$

$$R(\theta,\phi) = R_0(1 + \beta_2[\cos\gamma Y_{2,0}(\theta,\phi) + \sin\gamma Y_{2,2}(\theta,\phi)])$$

$$\rho_2 \propto -\cos(3\gamma)\beta_2^3$$

Could isolate the γ dependence

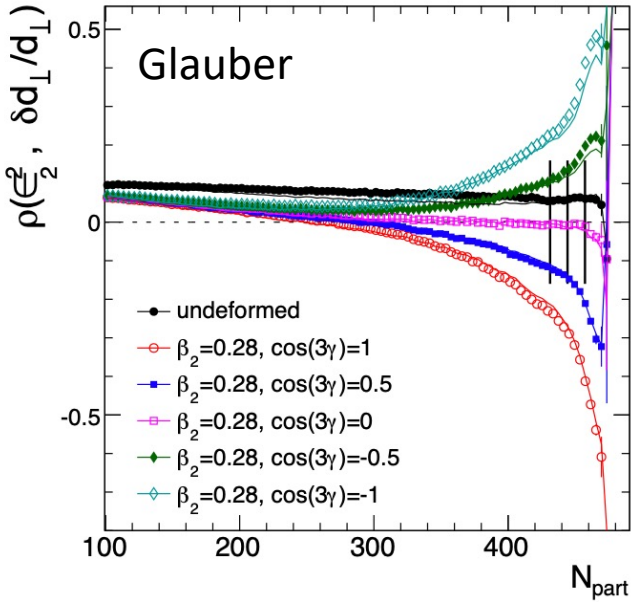

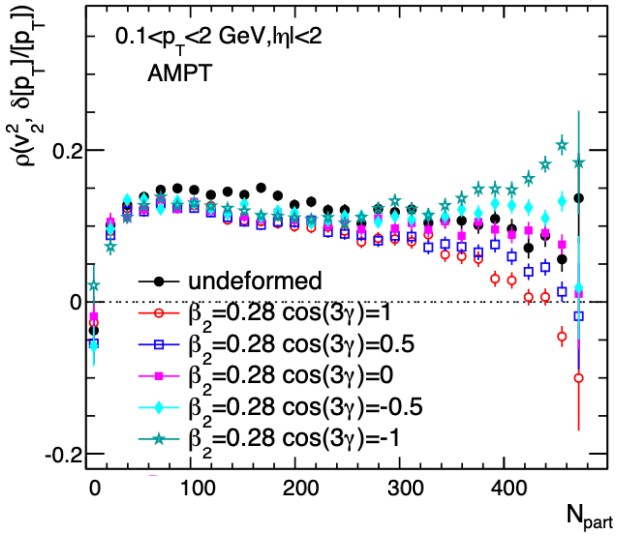

B. Bally et al., PRL 128, 082301 (2022)

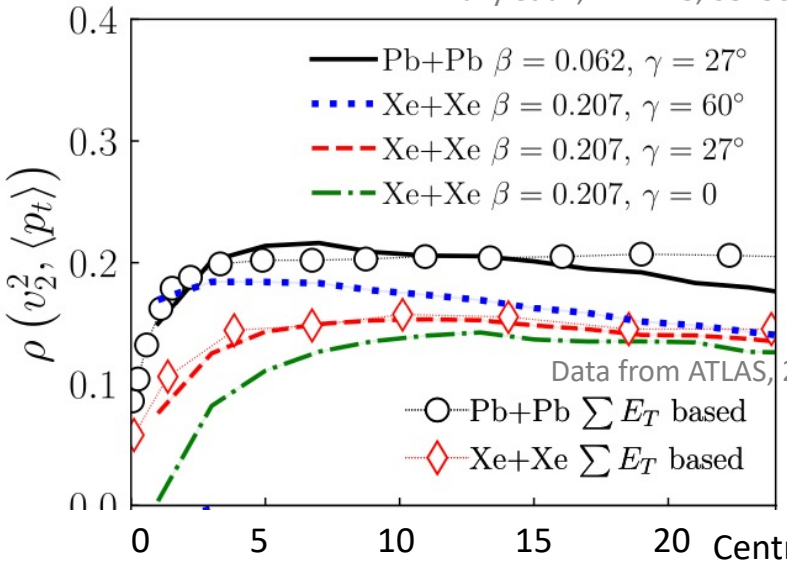

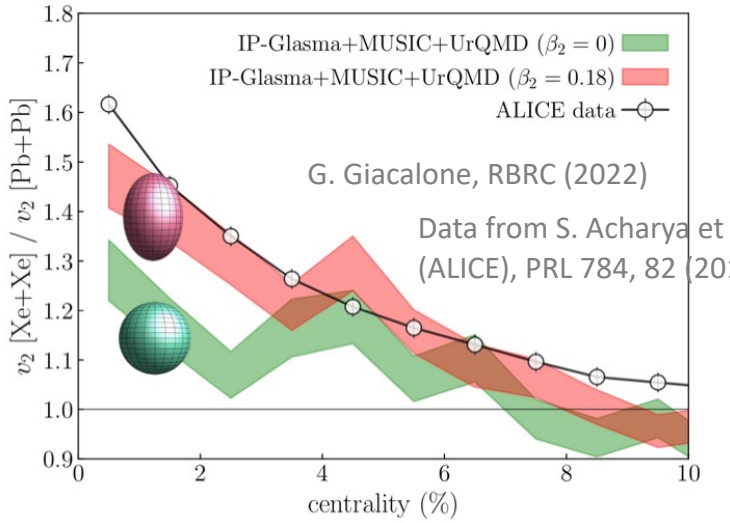

^{129}Xe also shows the quadrupole shape

Signature of the triaxial deformation at LHC

ATLAS, 2205.00039

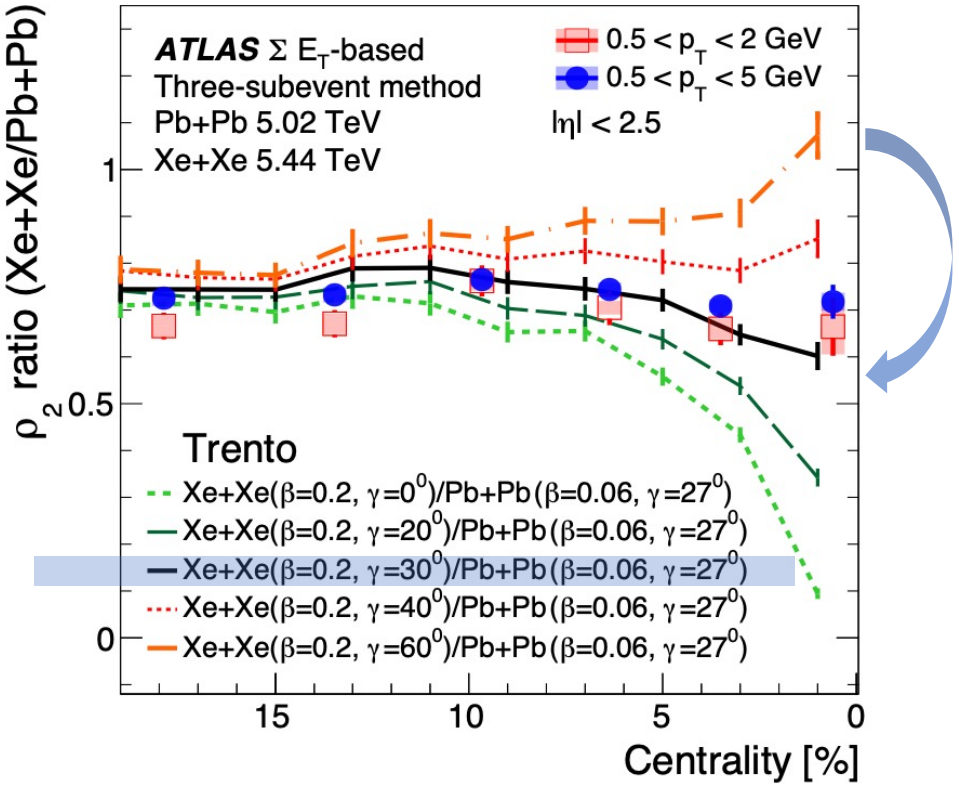

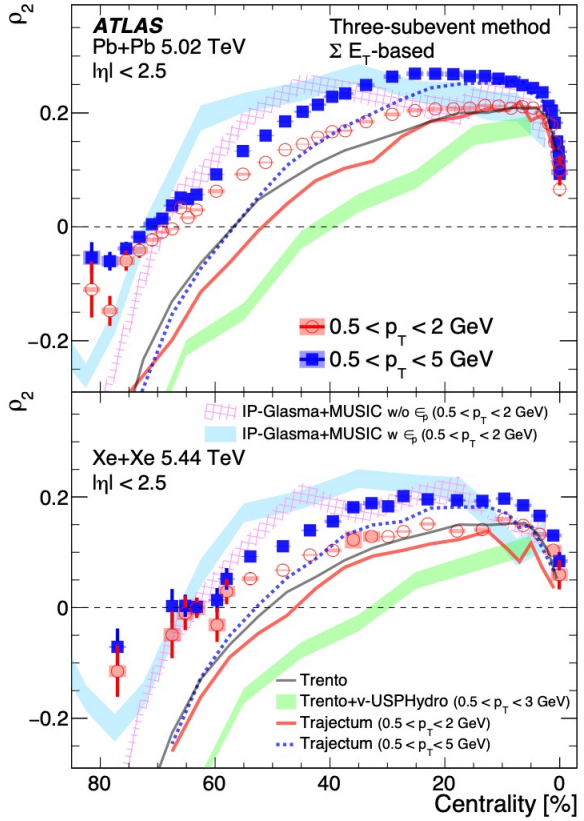

ALICE, PLB 834, 137393 (2022)

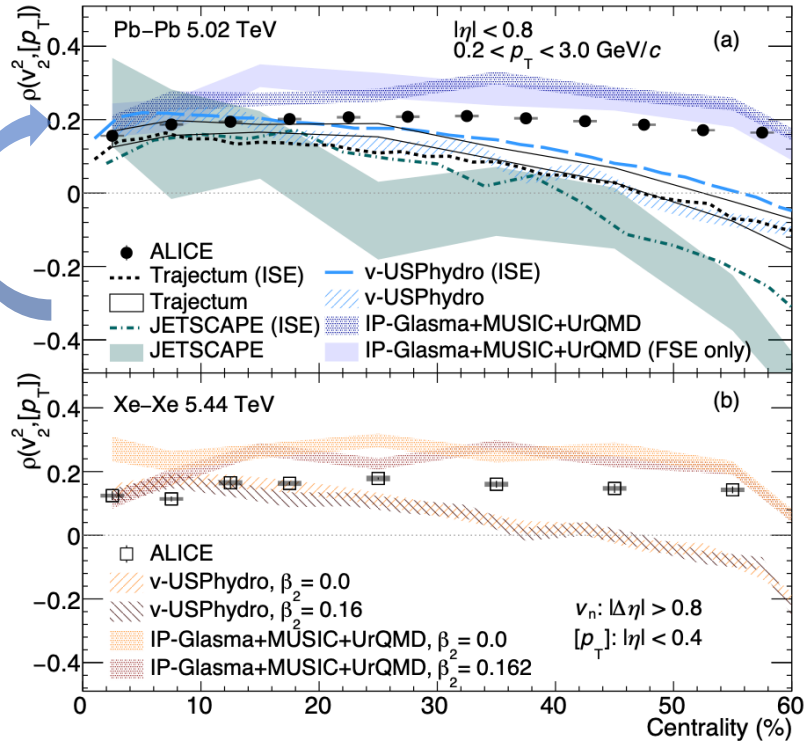

Multiple ways to deposit energy

$$e(x,y) \sim \begin{cases} T_A + T_B & N_{\text{part}} - \text{scaling}, p = 1 \\ T_A T_B & N_{\text{coll}} - \text{scaling}, p = 0, q = 2 \\ \sqrt{T_A T_B} & \text{Trento default}, p = 0 \\ \min\{T_A, T_B\} & \text{KLN model}, p \sim -2/3 \\ T_A + T_B + \alpha T_A T_B & \text{two-component model,} \\ & \text{similar to quark-glauber model} \end{cases} \qquad T \propto \left(\frac{T_A^p + T_B^p}{2} \right)^{q/p}$$

No p_T dependence, medium effect was canceled.

Confirm the triaxial shape of ^{129}Xe nuclei

- Pave a novel way to characterize the initial state

Nuclear structure in unique isobar ^{96}Ru and ^{96}Zr at RHIC

$$\rho(r,\theta,\phi) = \frac{\rho_0}{1+e^{(r-R(\theta,\phi))/a_0}}$$

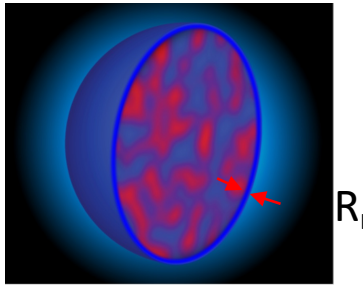

$$R(\theta,\phi) = R_0(1+\beta_2[\cos\gamma Y_{2,0}(\theta,\phi)+\sin\gamma Y_{2,2}(\theta,\phi)]+\beta_3 Y_{3,0}(\theta,\phi))$$

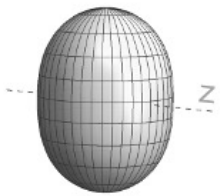

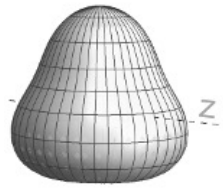

Signatures of nuclear structure in isobar collisions?

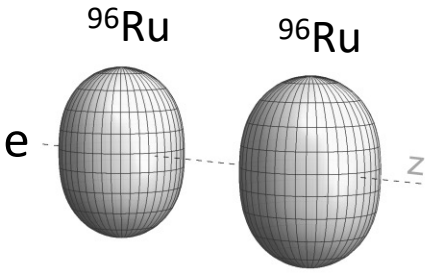

Quadrupole

$\beta_2 = 0.154$
$\beta_3 \sim 0$

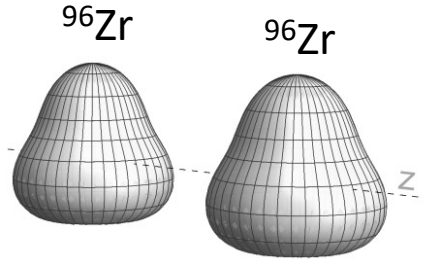

Octupole

$\beta_2 = 0.06$
$\beta_3 = 0.20 - 0.27$

Nuclear structure experimental data on Ru/Zr β_n:

	β_2	$E_{2_1^+}$ (MeV)	β_3	$E_{3_1^-}$ (MeV)
^{96}Ru	0.154	0.83	-	3.08
^{96}Zr	0.062	1.75	0.202,0.235,0.27	1.90

$$\beta_2 = \frac{4\pi}{3ZR_0^2}\sqrt{\frac{B(E2)\uparrow}{e^2}} \qquad \beta_3 = \frac{4\pi}{3ZR_0^3}\sqrt{\frac{B(E3)\uparrow}{e^2}}$$

G. Giacalone, J. Jia and V. Soma, PRC 104, L041903(2021)
J. Jia, PRC 105, 014905(2022); C. Zhang and J. Jia, PRL 128, 022301(20222)

M. S. Abdallah et al. (STAR), PRC 105, 014901(2022)

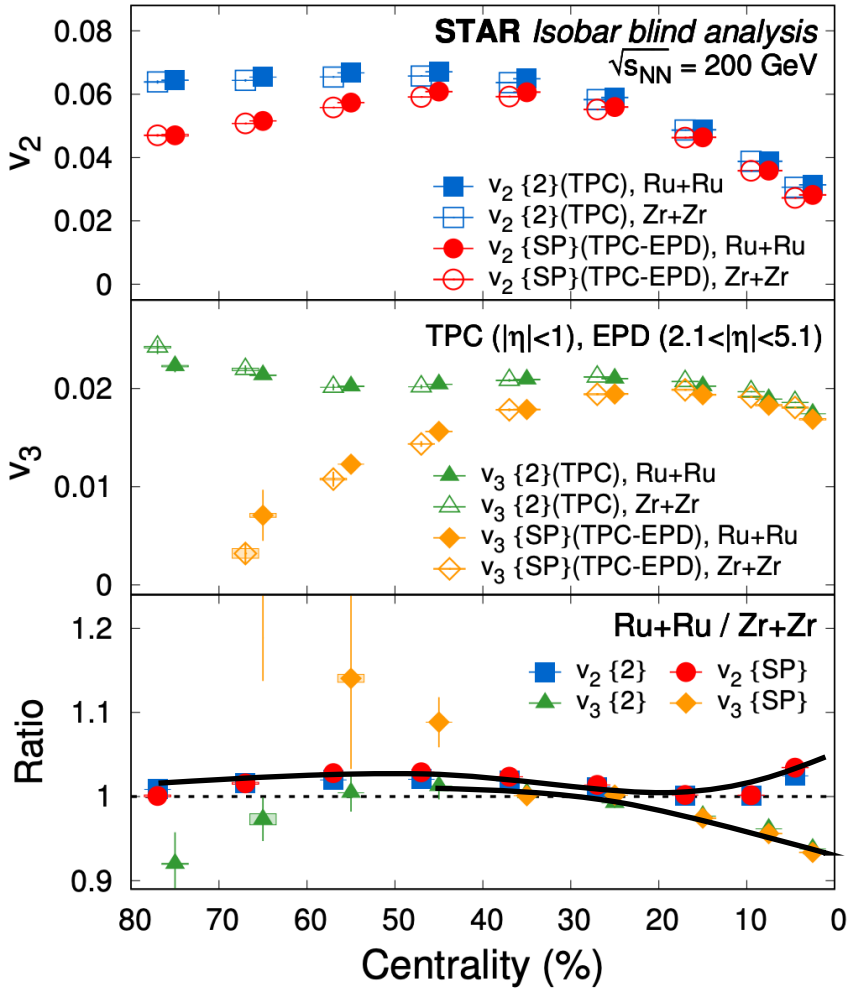

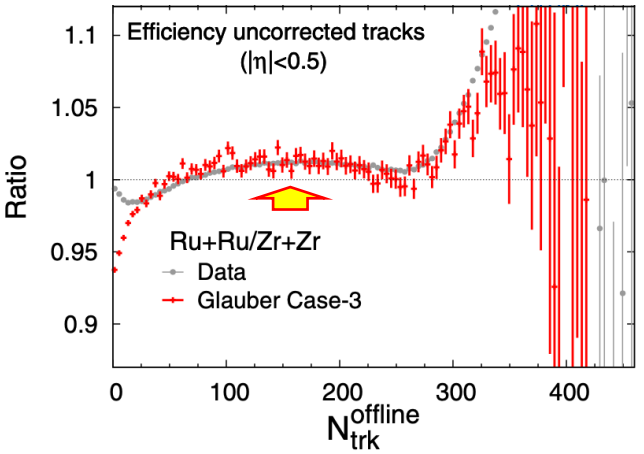

	Case-3 [113]		
Nucleus	R (fm)	a (fm)	β_2
$^{96}_{44}$Ru	5.067	0.500	0
$^{96}_{40}$Zr	4.965	0.556	0

$$\frac{\mathcal{O}_{X+X}}{\mathcal{O}_{Y+Y}} \overset{?}{=} 1$$

Significant departure from one

Nuclear deformation and neutron skin thickness via v_n ratio

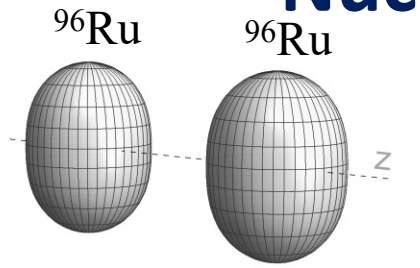

$R = 5.09$ fm
$a_0 = 0.46$ fm
$\beta_2 = 0.162$
$\beta_3 \sim 0$

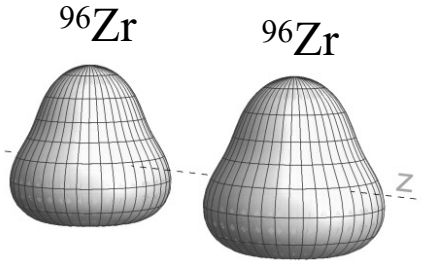

$R = 5.02$ fm
$a_0 = 0.52$ fm
$\beta_2 = 0.06$
$\beta_3 = 0.20 - 0.27$

J. Jia, PRC 105, 014905(2022

C. Zhang and J. Jia, PRL 128, 022301(20222)

Heavy-ion expectation:

$$v_2^2 = a_2 + b_2\beta_2^2 + b_{2,3}\beta_3^2, \quad v_3^2 = a_3 + b_3\beta_3^2$$

$$\frac{v_{2,\mathrm{Ru}}^2}{v_{2,\mathrm{Zr}}^2} \approx 1 + \frac{b_2}{a_2}\left(\beta_{2,\mathrm{Ru}}^2 - \beta_{2,\mathrm{Zr}}^2\right) - \frac{b_{2,3}}{a_2}\beta_{3,\mathrm{Zr}}^2$$

$$\frac{v_{3,\mathrm{Ru}}^2}{v_{3,\mathrm{Zr}}^2} \approx 1 - \frac{b_3}{a_3}\beta_{3,\mathrm{Zr}}^2 < 1$$

Cancelation expected in non-central collisions

Q. Shou, Y.G. Ma et al., PLB 749,215(2015)

H.L. Li and H.J. Xu et al., PRC 98.054907(2018)

H.J. Xu et al., PLB 819, 1136453(2021)

G. Giacalone, J. Jia and V. Soma, PRC 104,L041903(2021)

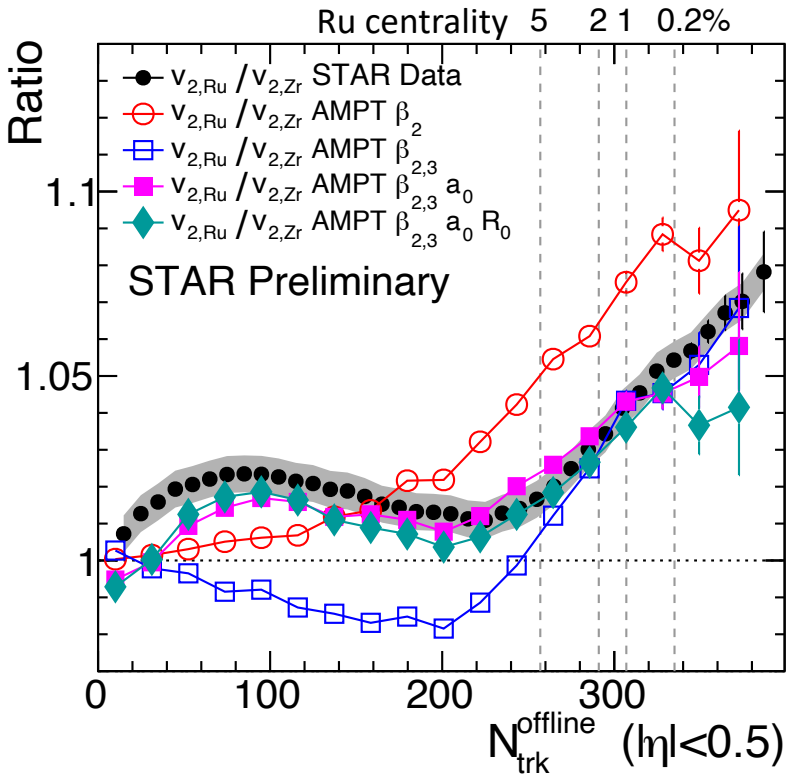

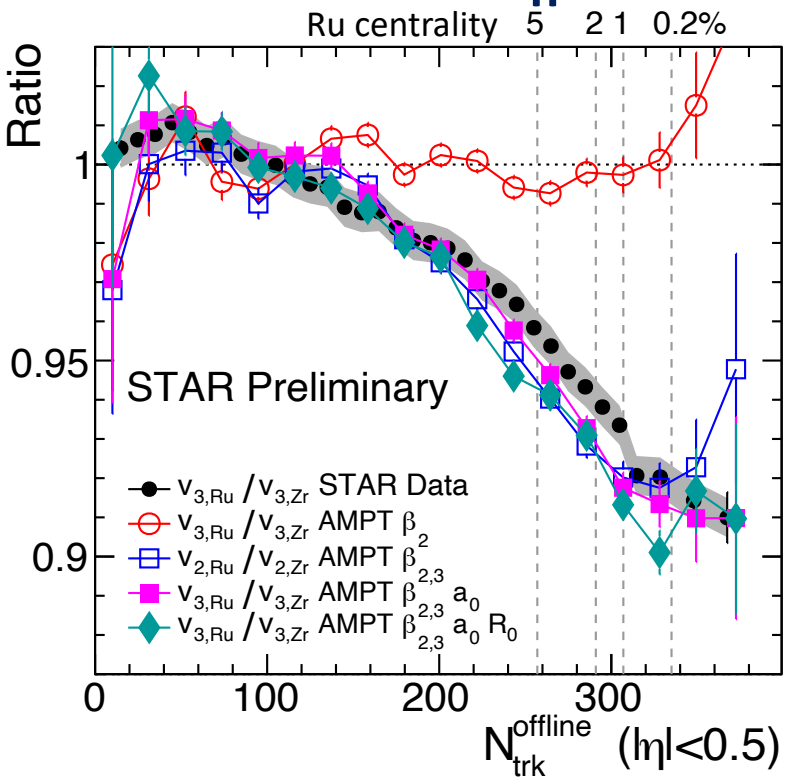

1) v_2 ratio: large $\beta_{2,\mathrm{Ru}}$, negative contribution from $\beta_{3,\mathrm{Zr}}$ ⇒ Sharper increase in central

2) v_3 ratio: strong decrease from $\beta_{3,\mathrm{Zr}}$ with negligible $\beta_{2,\mathrm{Ru}}$ distortion

3) Residual effect due to radial structure, e.g., neutron skin in Zr

4) No significant effect due to nuclear size

✓ The large differences of v_2 and v_3 suggest $\boldsymbol{\beta_{2,\mathrm{Ru}} \gg \beta_{2,\mathrm{Zr}}}$ **and** $\boldsymbol{\beta_{3,\mathrm{Ru}} \ll \beta_{3,\mathrm{Zr}}}$.

Direct indication of octupole deformation in heavy-ion collisions.

Nuclear deformation via $[p_T]$ variance ratio

J. Jia, PRC 105, 014905(2022)

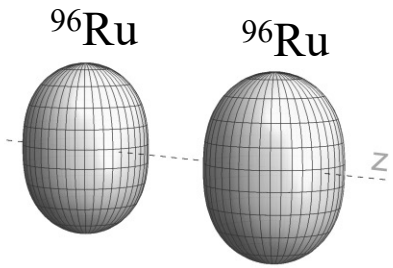

$R = 5.09$ fm
$a_0 = 0.46$ fm
$\beta_2 = 0.162$
$\beta_3 \sim 0$

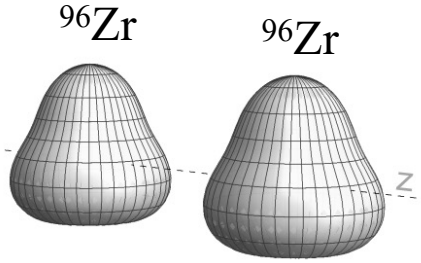

$R = 5.02$ fm
$a_0 = 0.52$ fm
$\beta_2 = 0.06$
$\beta_3 = 0.20 - 0.27$

Heavy-ion expectation:

$$\left\langle (\delta[p_T]/[p_T])^2 \right\rangle = a_0 + b_0\beta_2^2 + b_{0,3}\beta_3^2$$

$$\frac{\langle \delta p_T^2 \rangle_{Ru}}{\langle \delta p_T^2 \rangle_{Zr}} \approx 1 + \frac{b_0}{a_0}\left(\beta_{2,Ru}^2 - \beta_{2,Zr}^2\right) - \frac{b_{0,3}}{a_0}\beta_{3,Zr}^2$$

Cancelation expected in non-central collisions

$$\left\langle (\delta[p_T]/[p_T])^2 \right\rangle \propto \left\langle (\delta d_\perp/d_\perp)^2 \right\rangle = \langle \delta_d^2 \rangle + \left\langle p_0(\Omega_1, \Omega_2, \gamma)^2 \right\rangle \beta_2^2$$

✓ $\beta_{2,Ru} \gg \beta_{2,Zr}$ and $\beta_{3,Ru} \ll \beta_{3,Zr}$.

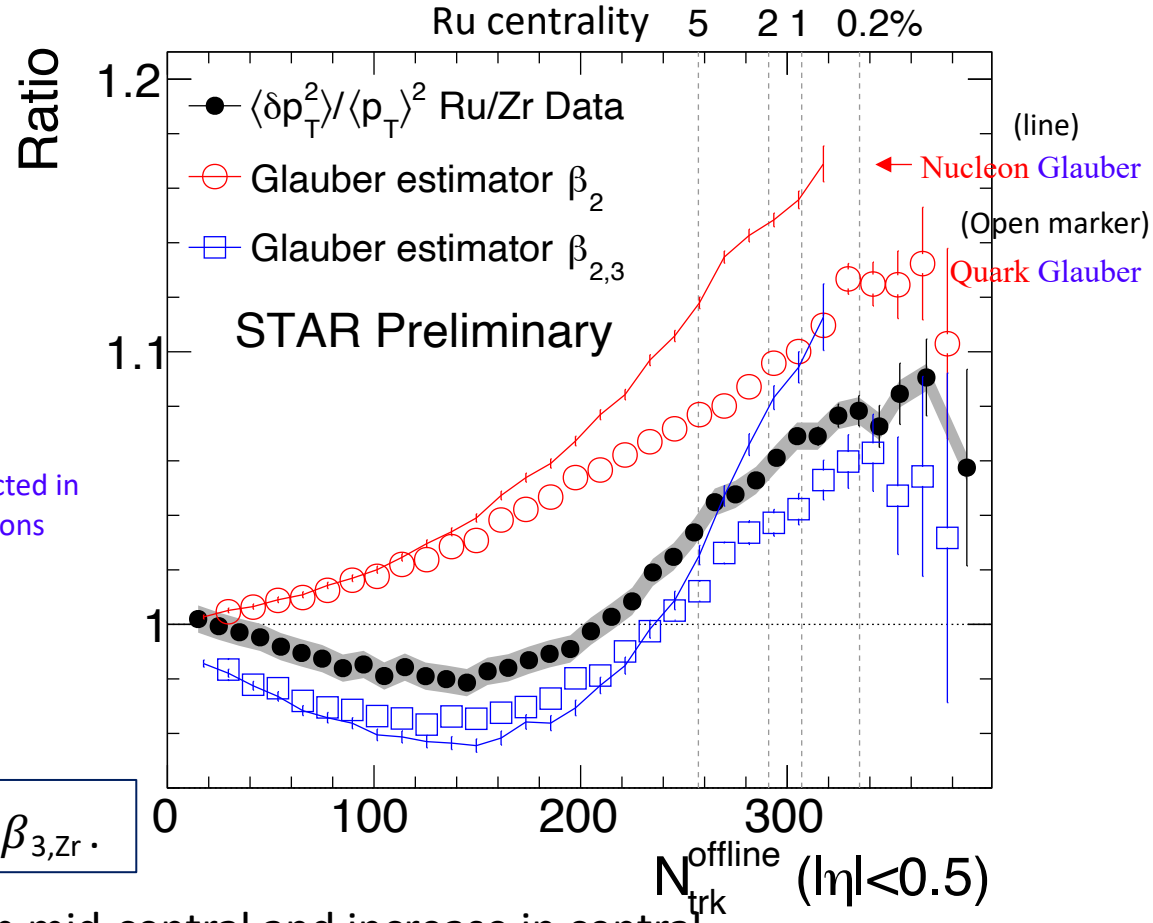

1) Nonmonotonic trend: large suppression in mid-central and increase in central

2) Enhancement from mid-central ⇒ large $\beta_{2,Ru}$

3) Large suppression in mid-central ⇒ strong octupole $\beta_{3,Zr}$

Variance of $[p_T]$ fluctuations can also be used to constrain the nuclear deformation.

Nuclear skin thickness via multiplicity ratio

J. Jia, PRC105, 014905(2022)

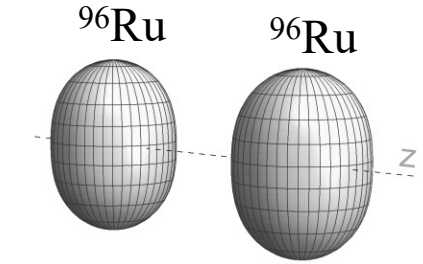

$R = 5.09$ fm
$a_0 = 0.46$ fm
$\beta_2 = 0.162$
$\beta_3 \sim 0$

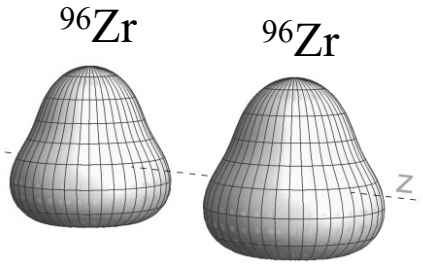

$R = 5.02$ fm
$a_0 = 0.52$ fm
$\beta_2 = 0.06$
$\beta_3 = 0.20 - 0.27$

M. S. Abdallah et al. (STAR), PRC105, 014901(2022)

Q. Shou, Y.G. Ma et al., PLB749, 215(2015)

H.L. Li and H.J. Xu et al., PRC98, 054907(2018)

H.J. Xu et al., PLB819, 1136453(2021)

J. Jia and C. Zhang, 2111.15559

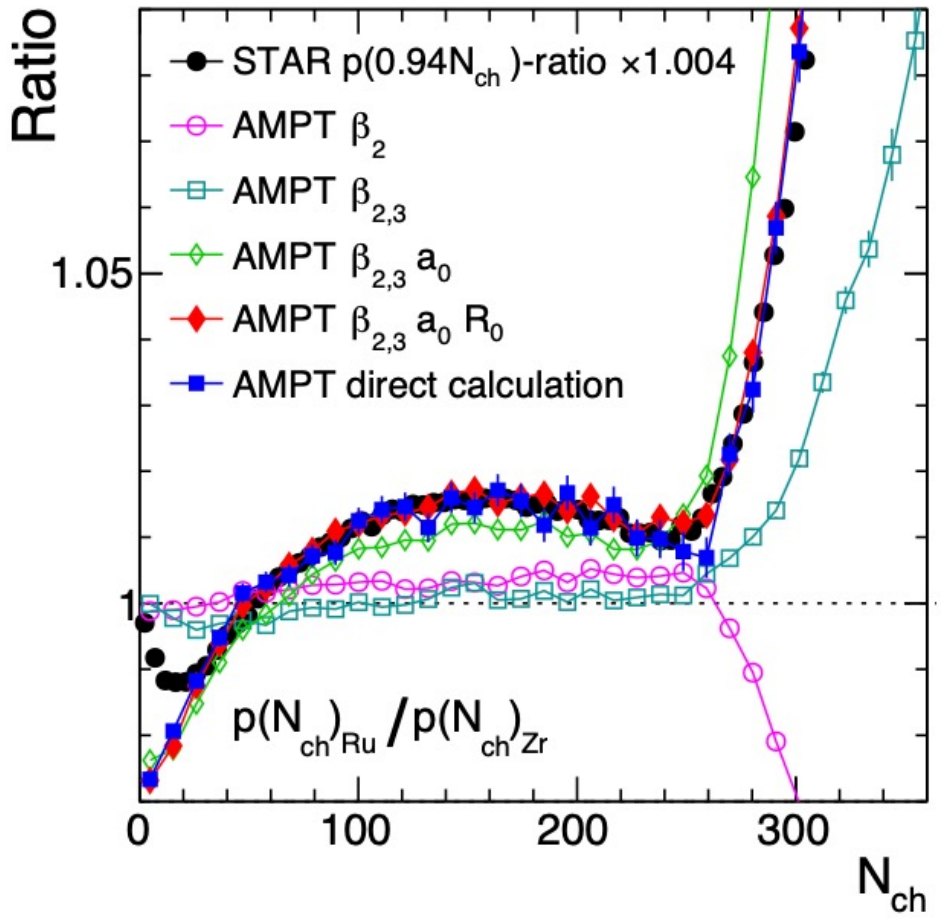

1) Nonmonotonic trend: bump in mid-central and increase in central

2) When only consider β_2 in case-1 and case-2: constant in peripheral and mid-central, but decrease in central.

3) But if you consider β_3 in Zr: also can almost get the same tail as Case-3.

4) Neutron skin a_0 dominates the bump in peripheral and mid-central. But the central tail is more tricky.

5) Nuclear size R also can affect the trend.

Nuclear skin thickness via multiplicity and [p_T] ratios

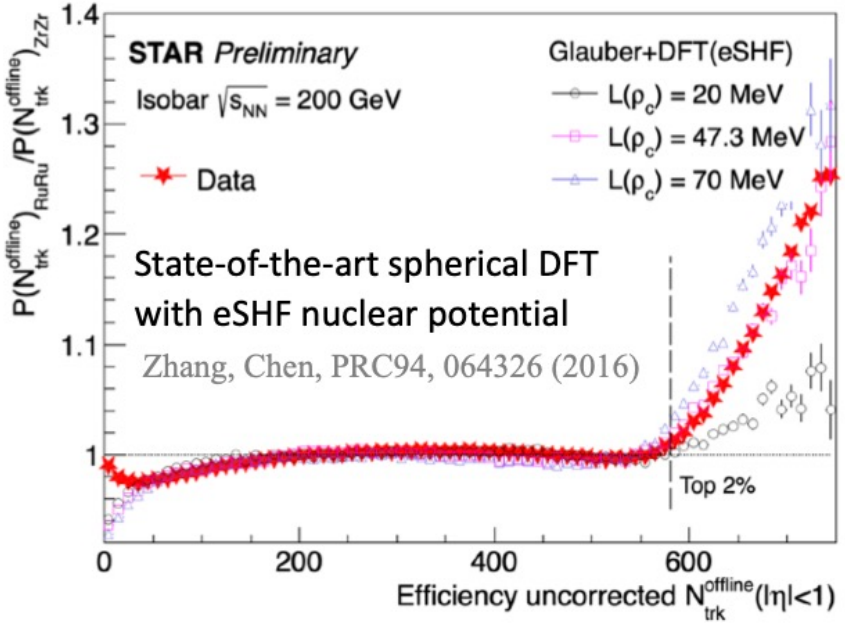

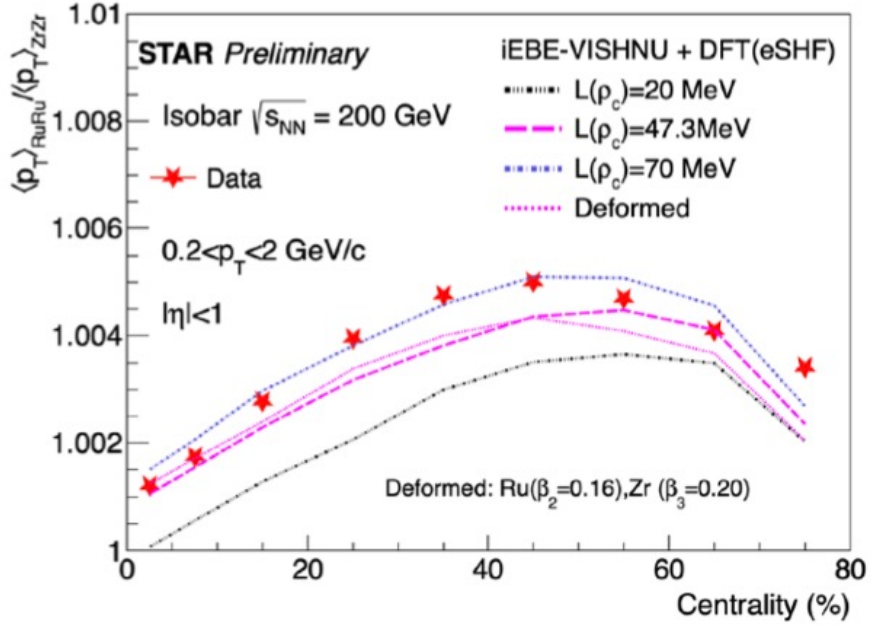

Plots from Haojie Xu

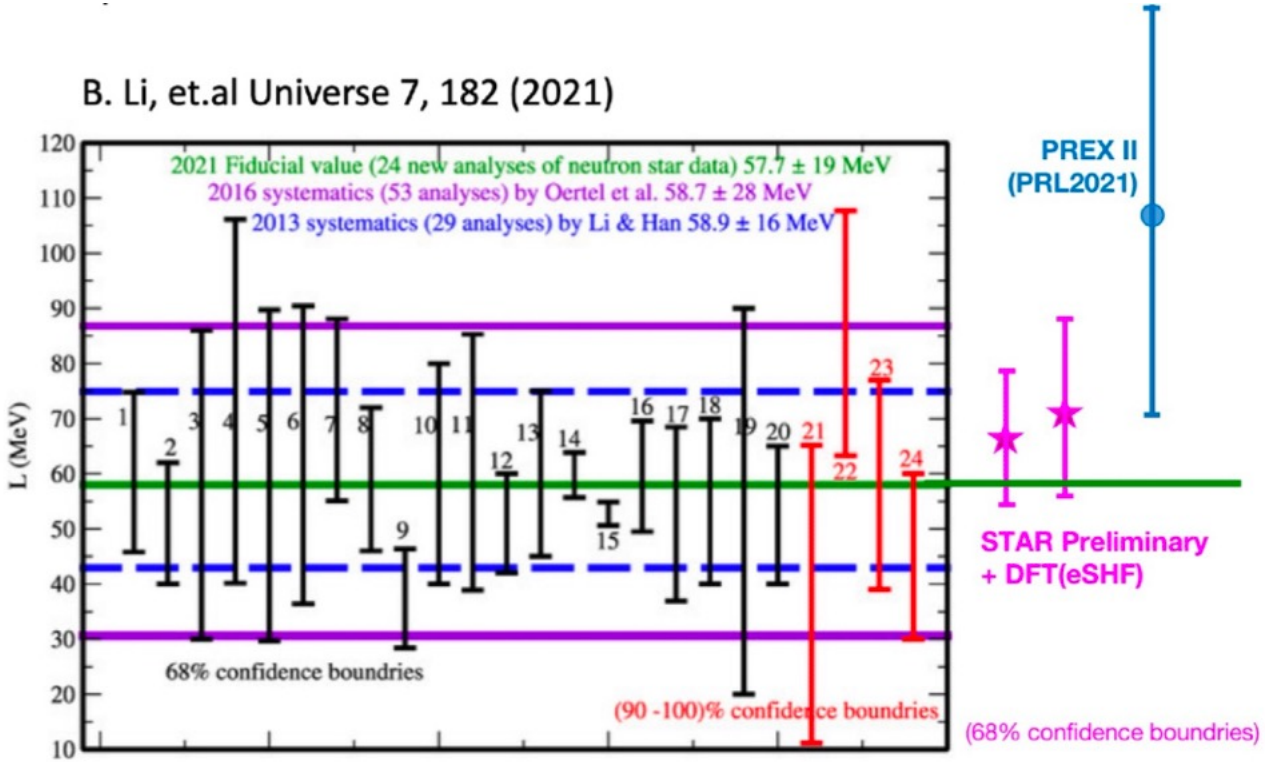

Constrain symmetry energy from heavy-ion view.

Another promising way: detect the neutron skin in ultra-peripheral collisions

—STAR, Science Advance 9, 3903 (2023)

Nuclear structure influence everywhere

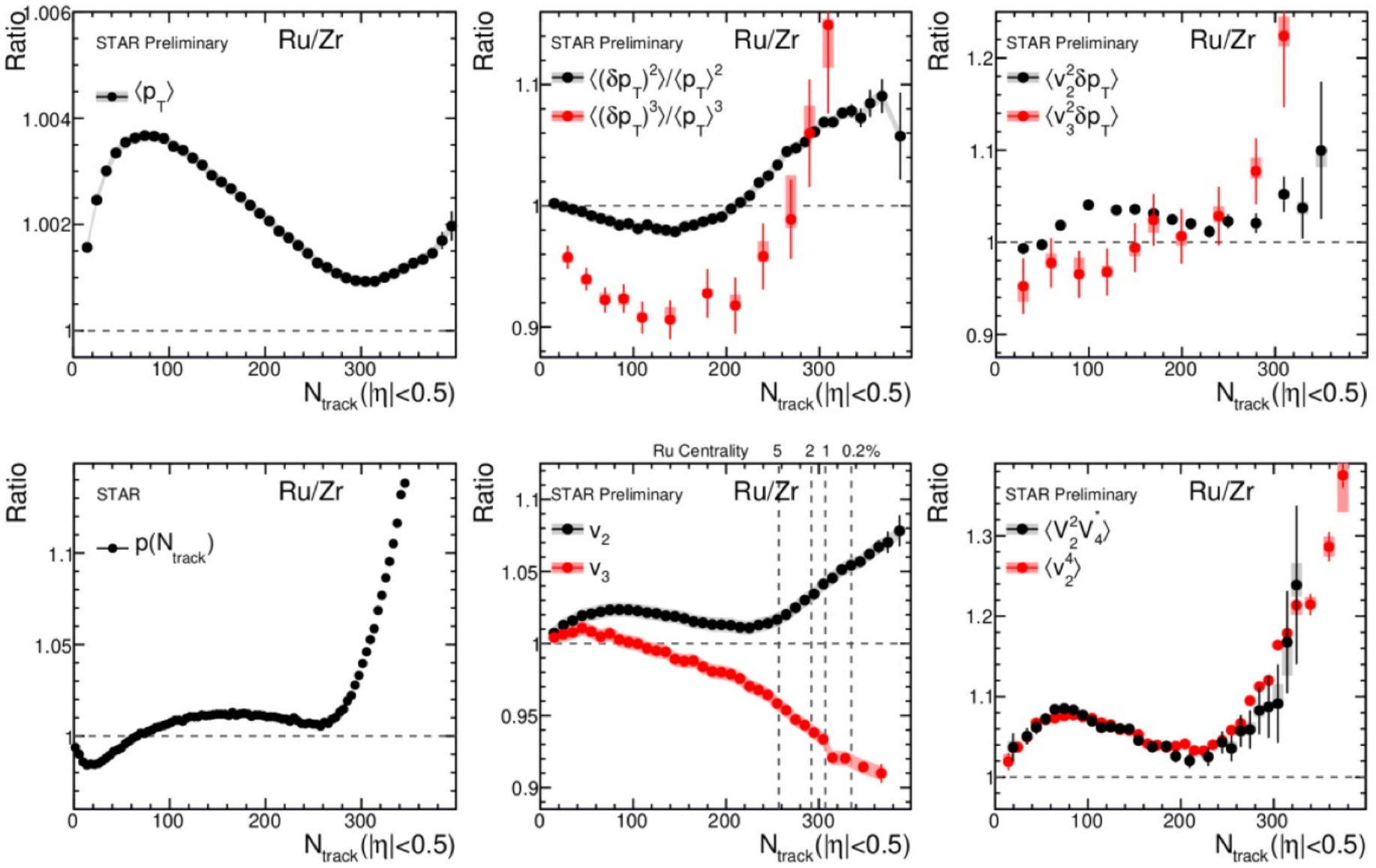

Future endeavors and opportunities

A:

$$\rho(r,\theta,\phi) = \frac{\rho_0}{1+e^{(r-R(\theta,\phi))/a_0}}$$

$$R(\theta,\phi) = R_0(1+\beta_2[\cos\gamma Y_{2,0}(\theta,\phi)+\sin\gamma Y_{2,2}(\theta,\phi)]+\beta_3 Y_{3,0}(\theta,\phi)+\beta_4 Y_{4,0}(\theta,\phi))$$

Indication of the octupole and hexadecapole in ^{238}U nuclei in heavy collisions

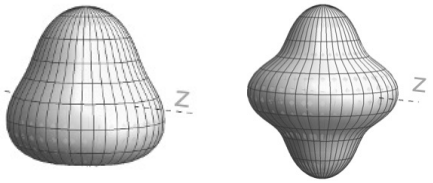

B: Light nuclei cluster at RHIC and LHC energy

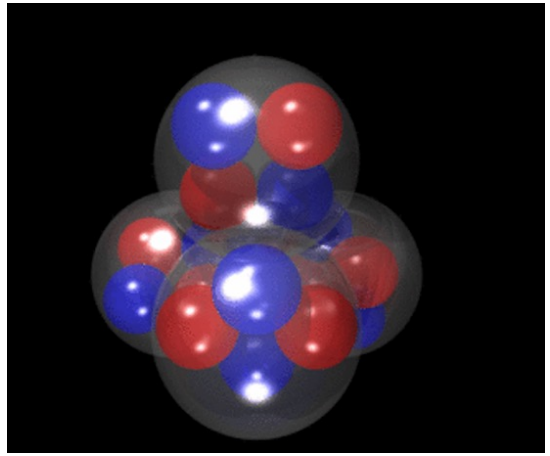

Single-Beam Energy (GeV/nucleon)	$\sqrt{s_{NN}}$ (GeV)	Run Time	Species	Events (MinBias)
100	200	1 week	O+O	400 M 200 M (central)
100	200	1 week	d+Au	100M MB 100M Central

(RHIC-STAR-RUN21 took all the data we wanted and more)

LHC: p+O and O+O collisions

C:

Strategy: constrain initial condition "independently" with nuclear structure input

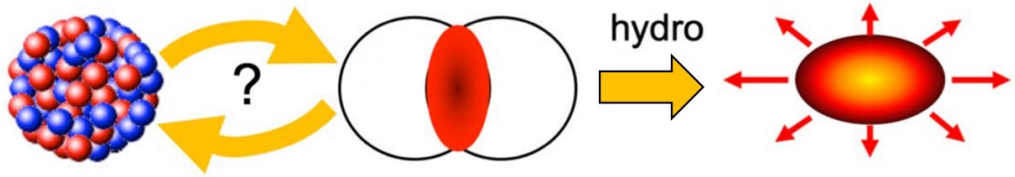

Multiple ways to deposit energy

$$T \propto \left(\frac{T_A^p + T_B^p}{2}\right)^{q/p}$$

$$e(x,y) \sim \begin{cases} T_A + T_B & N_{\text{part}} - \text{scaling}, p = 1 \\ T_A T_B & N_{\text{coll}} - \text{scaling}, p = 0, q = 2 \\ \sqrt{T_A T_B} & \text{Trento default}, p = 0 \\ \min\{T_A, T_B\} & \text{KLN model}, p \sim -2/3 \\ T_A + T_B + \alpha T_A T_B & \text{two-component model,} \\ & \text{similar to quark-glauber model} \end{cases}$$

From Jiangyong Jia

W.B. He, Y.G. Ma et al., PRL113, 032506(2014); W. Broniowski and E.R. Arriola, PRL112, 112501(2014); P. Bozek et al., PRC90, 064902(2014); S. Zhang, Y.G. Ma et al., PRC95, 063904(2017);

Conclusions and Outlooks

1. The signatures of nuclear deformation in heavy-ion collisions are everywhere and robust:
   quadrupole, octupole, hexadecapole, and triaxiality deformations
   neutron skin thickness

2. Decoding the nuclear structure can be done via many tools:
   Bulk observables: flow v_n, v_n-[p_T] correlations, N_{ch}, $\langle p_T \rangle$ and it's fluctuations
   Ultra-peripheral collisions

3. The signals could be qualitatively described by the hydrodynamics and transport models:
   It helps us to further understand and better treat initial conditions.

4. Isobar collisions are the new and best tools to quantify nuclear structure:
   final state effects are canceled by ratios.

5. The best and most appropriate opportunity for us to open up the interdisciplinary connection between low-energy and high-energy connections.

6. RHIC/LHC O+O runs could potentially help to decipher cluster structures in our future steps.

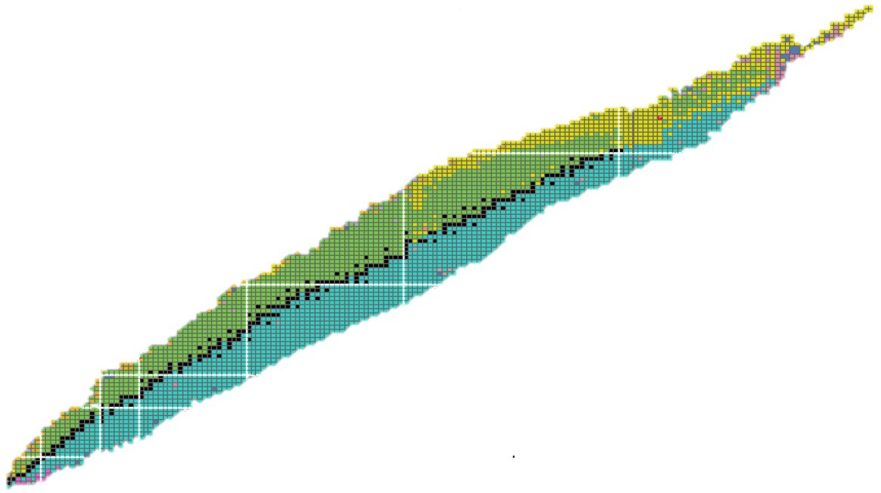

Low energy community

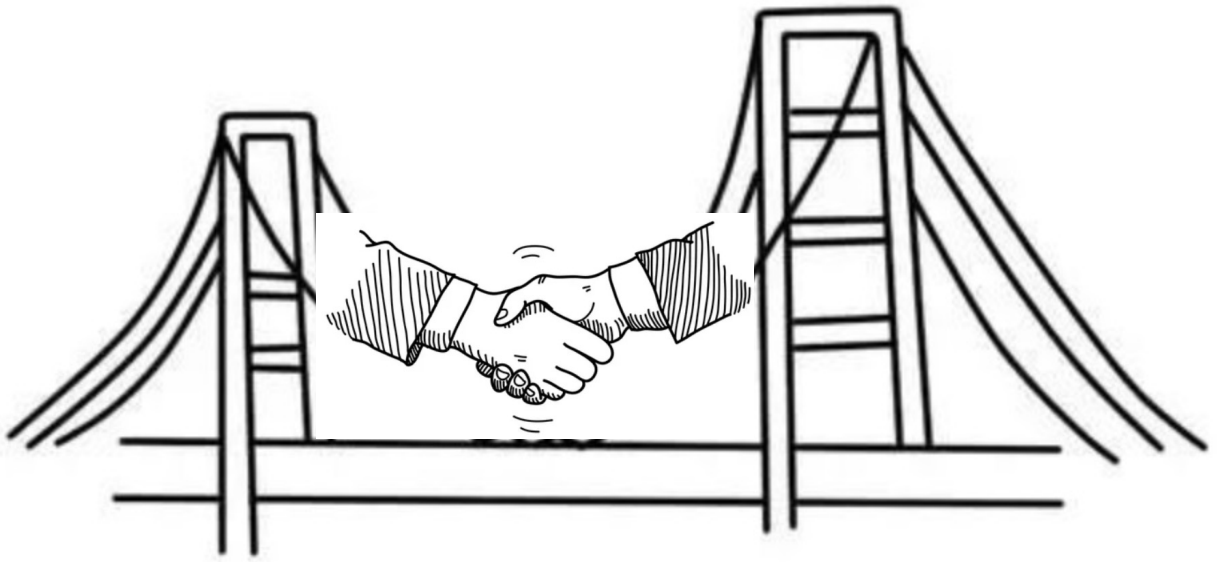

Heavy-ion community

Detect the neutron skin in ultra-peripheral collisions

STAR, Science Advance 9, 3903 (2023)

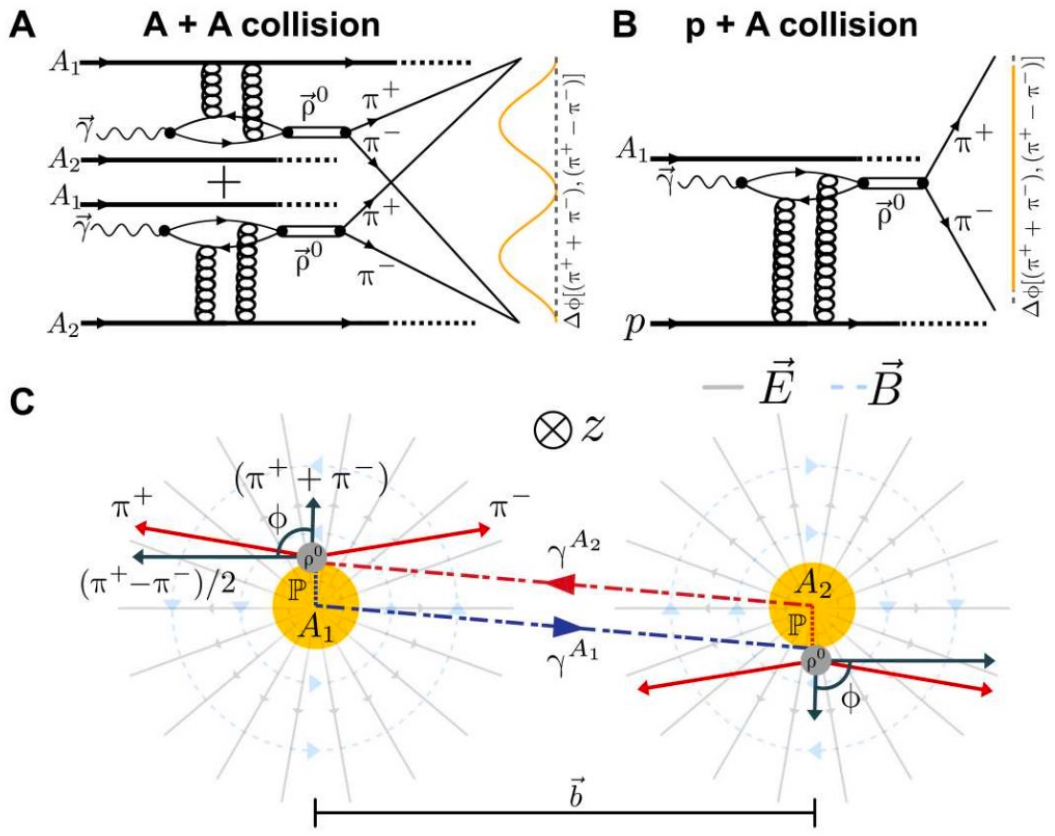

$$f(t) = A_c |\mathcal{F}[\rho_A(r;R,a)](|t|)|^2 + \frac{A_i/Q_0^2}{(1+|t|/Q_0^2)^2} \qquad \rho_A(r;R,a) = \frac{\rho_0}{1+\exp[(r-R)/a]}$$

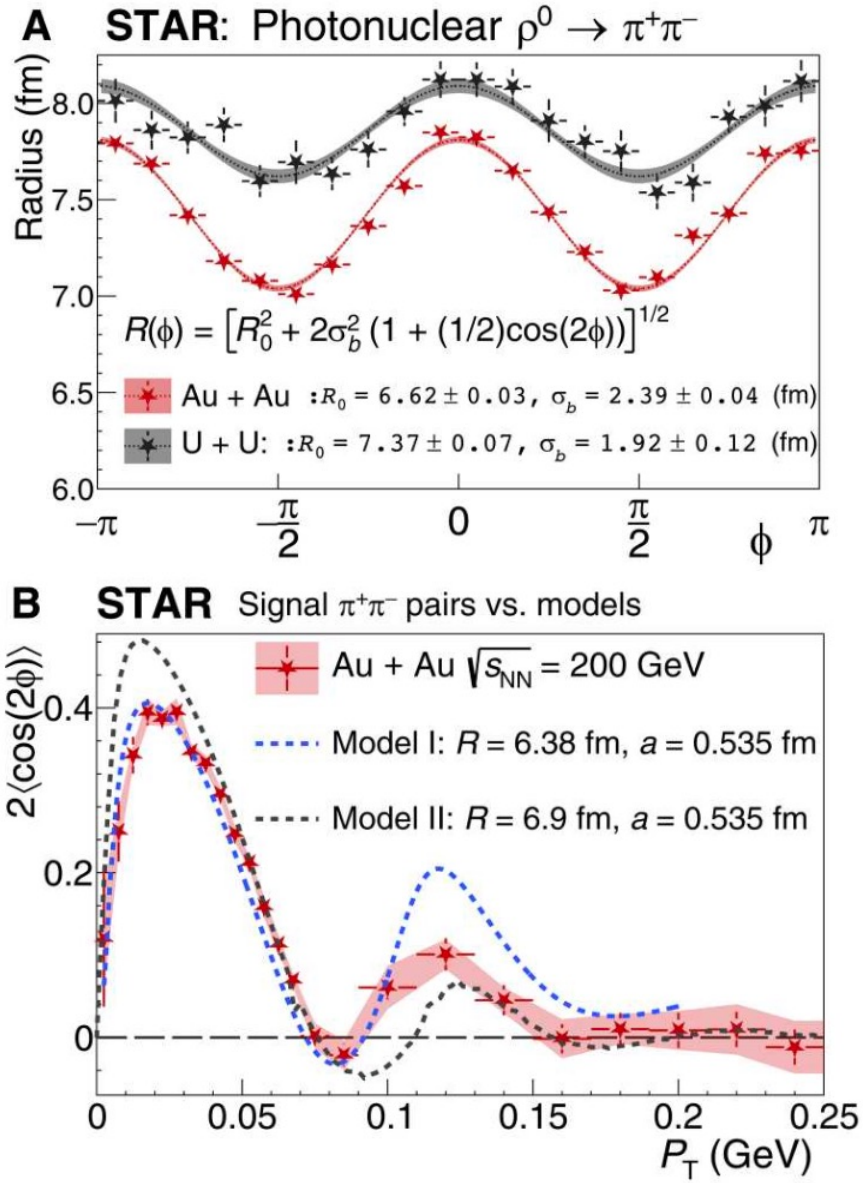

R_{Au} = 6.53 ±0.03 (statistical) ±0.05 (systematic)
R_U = 7.29 ± 0.06 (statistical) ±0.05 (systematic)

$\Delta R_{Au} = R_n - R_p = 0.17 \pm 0.03$ (statistical)±0.08 (systematic) fm
$\Delta R_U = R_n - R_p = 0.44 \pm 0.05$ (statistical)±0.08 (systematic) fm